

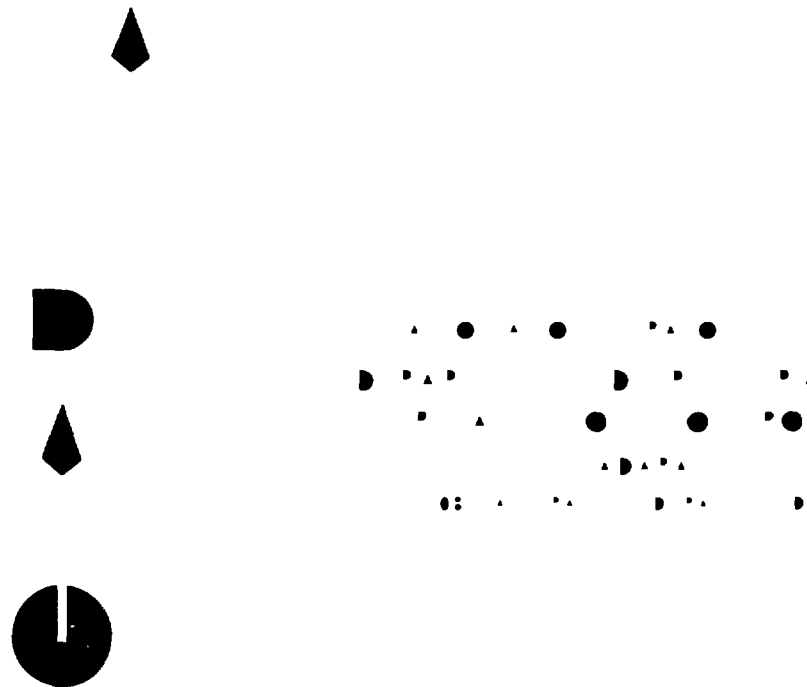
DRFC/CAD

EUR-CEA-FC-1390

SCATTERING MATRIX OF TORE SUPRA  
LOWER HYBRID ANTENNA

Ph. Bibet, J. Achard, G. Berger By, M. Goniche, R. Magne,  
J.J. Capitain, G. Rey, G. Tonon, X. Litaudon, D. Moreau

Mars 1990



SCATTERING MATRIX OF TORE SUPRA LOWER HYBRID ANTENNA

Ph. BIBET - J. ACHARD

AND

G. BERGER BY - M. GONICHE - R. MAGNE - J.J. CAPITAIN

G. REY - G. TONON - X. LITAUDON - D. MOREAU

- 1 - PRESENTATION OF TORE SUPRA LOWER HYBRID ANTENNA
  - 1.1 - Introduction
  - 1.2 - A module
    - 1.2.1 - 3 dB coupler
    - 1.2.2 - Phase shifter
  
- 2 - THEORETICAL COMPUTATION OF THE ANTENNA SCATTERING MATRIX
  - 2.1 - Definition and properties of the scattering matrix (SM)
    - 2.1.1 - Definition
    - 2.1.2 - Properties
    - 2.1.3 - Size of the matrix
  - 2.2 - Computation of a half a module SM
  - 2.3 - Computation of a module SM
    - 2.3.1 - Remarks
  - 2.4 - The antenna SM
  - 2.5 - Results
    - 2.5.1 - Module prototype
      - 2.5.1.1 - With a load
      - 2.5.1.2 - with a short circuit
    - 2.5.2 - Module 0
      - 2.5.2.1 - 10 x 10 Matrix
    - 2.5.3 - The antenna scattering matrix
  
- 3 - EXPERIMENTAL MEASUREMENT OF A MODULE SM
  - 3.1 - Measurement method
    - 3.1.1 - Exciting magnetic probe
    - 3.1.2 - Smaller size waveguide coupler
    - 3.1.3 - Accuracy

### 3.2 - Results

3.2.1 - 9 x 9 SM of the prototype

3.2.1.1 - With a load

3.2.1.2 - With a short circuit

3.2.2 - 10 x 10 SM of the module 0

### 4 - USE OF THE SM

4.1 - Observation of the behavior of the antenna  
in front of the plasma

4.2 - Computation of the coupling coefficients and the  
real N// spectra

### 5 - CONCLUSION

## 1 - PRESENTATION OF TORE SUPRA LOWER HYBRID ANTENNA

### 1.1 - Introduction

For lower hybrid current drive and mode stabilization [1] 8 MW of CW 3.7 GHz RF power are to be injected in TORE SUPRA ( $I_p = 1.7$  MA,  $a = 75$  cm).

This will be done by the use of 2 antennas fed by 16 TH 2103 500 kW CW klystrons.

The couplers are designed to inject a wave with a  $N//$  of 1.9. This is realized by choosing the distance and the incident wave phase shift between each neighbouring waveguide. For TORE SUPRA these values are 10 mm and  $90^\circ$ . The first one is fixed, the other can be changed because the phase shift between each klystron can be monitored by an INTEL 80386 computer.

Due to the huge incident power necessary to drive the current in such a machine as TORE SUPRA, it is no more possible to have one vacuum window for each waveguide arriving in front of the plasma because the total number of waveguides is high. This is due to the multipactor limitation which implies that the power density under vacuum must be below  $5$  kW/cm<sup>2</sup>. One antenna is therefore made of 16 modules for which there is one vacuum window and 8 output waveguides in front of the plasma. They are set in 2 horizontal rows of 8 modules. That means that in front of the plasma there is a "grill" of 4 horizontal rows of 32 waveguides [2] (photo 1).

These modules are not identical. There are 4 main families. The change between them is mainly due to the whole geometry of the coupler. Due to a lack of space, the 2 neighbouring modules on the same horizontal line are reversed. The coupler has also a poloidal shape in front of the plasma : therefore the electric length of 2 waveguides on the same vertical line is not the same.

When the geometry of the antenna is chosen, it is necessary to know its RF behavior. That means it is necessary to know the incident and the reflected fields in each waveguide when some of them are known. To solve this problem, the relations which link each electric field to the others are given by the knowledge of the scattering matrix of the antenna.

There are two ways to find the scattering matrix :

- The first one is to calculate it. The first step is to compute the SM of half a module. Then the one of a module in its entirety. When this has been done for every type of modules, the SM of the coupler can be deduced.

- The second one is to measure it.

The two methods have been performed for TORE SUPRA lower hybrid heating antenna. Therefore the experimental and the theoretical SM can be compared. One can see further that they are in a quite good agreement.

Then when the SM has been obtained it can be used for many purposes. Two only have been studied there.

The first one is to use it to really observe the behavior of the antenna in front of the plasma to see if no breakdown is occurring under vacuum due to the multipactor effect. With the knowledge of the electric field measured at the end of each output waveguide and of the scattering matrix of the coupler, the reflexion coefficient at the input of each module can be compared to the experimental one.

In front of the plasma there is a coupling between each waveguide and its neighbours. Unfortunately there are no measurements on each output waveguide. But there is a bidirectional coupler at the input of each module to know the incident and the reflected waves. Therefore the coupling coefficient between each module and its neighbours can be determined. It can then be compared to the one obtained by using the scattering matrix of the antenna and the plasma admittance matrix given theoretically by the code SWAN (Slow Wave ANTenna) for a given electronic density and for a given density gradient. The real  $N//$  spectra can then be computed. These two items are considered further.

#### 1.2 - A module

Each module has one input port and 8 output ports in front of the plasma set in two horizontal lines of 4 waveguides [2]. At the input one can find :

First a bidirectional coupler with a coupling of 50 dB for the incident wave and 40 dB for the reflected wave. The directivity is better than 40 dB.

Then there is a DC break to insulate the transmission line from the machine whose voltage may accidentally reach a value of 1 kV.

It is followed by a water cooled quarter wavelength pillbox type vacuum window protected by an arc detector. This item is the boundary between the atmospheric pressure inside the transmission line and the vacuum inside the machine.

At last there is the part in the vacuum. Because the module must withstand 250 kW continuous wave, this one is made of copper and water cooled at a temperature of 230°.

The input waveguide is divided into 2 by using a 3 dB coupler. Then to compensate the 90° phase shift due to the hybrid junction, a phase shifter (p.s.) is put in the output waveguide to accelerate the wave which is late compared to the other output waveguide in order to have 0° phase shift between 2 vertical waveguides at the mouth of the module. In fact its value is different from 90° because it takes into account the antenna mouth poloidal shape.

Then each output waveguide is divided into 2 on the shorter side. A 180° p.s. is put on the 2nd waveguide taking into account the direction of the spectra compared to the plasma current. The incident wave phase value is decreasing in the direction of the electron velocity. Then the two waveguides are also divided into 2 and a 90° p.s. is added. By this way a 90° incident wave phase shift is obtained between each neighbouring waveguide (fig. 1).



On the balance port of the 3 dB coupler there is no incident power therefore it will see only the reflected field. To prevent from RF leakage a short circuit or a load must be put. The estimated RF reflected power in bad density conditions for the coupling of the wave with the plasma has been limited to 50 kW CW. Only a water cooled load can withstand such an energy. The problem is that it is difficult to put under vacuum a water load on each module which can withstand 50 kW CW. It is easier to put a short circuit, but this choice implies that the coupling between the two output ports of the hybrid junction is higher. Another aim of this study is to see the difference between the 2 solutions.

Before to realize the antennas 2 first modules have been made : a module prototype and a module labeled 0. The dimensions of the input port are 34 x 76 (mm x mm). For the 8 output waveguides the larger size is the same than for the input port, the shorter one is 6.75 mm for the module prototype and 8.5 mm for the module 0. The wall thicknesses are respectively 3 and 2 mm. For the antenna the dimensions are the same than for module 0. The phase shift has been geometrically fixed between 2 neighbouring waveguides on the same vertical line at 0° and 90° on the same horizontal line for the incident wave.

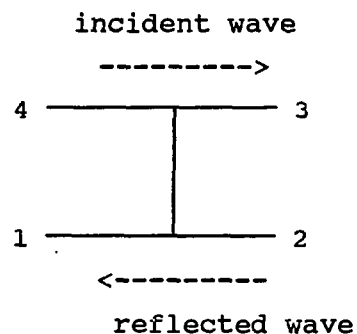
To realize the whole antenna there are, as said previously, 4 different modules labeled 1H, 1B, 2H, 2B. Due to the poloidal shape the phase shifter on one output of the 3 dB coupler has a value of  $135^\circ$  for the 1H and 2B type and  $45^\circ$  for the others. These values are different from  $90^\circ$  due to the poloidal shape which leads to an electric length change of  $45^\circ$ . The module 1H total electric length is different from the module 2B one because the  $34 \times 76$  (mm x mm) part which is between the vacuum window and the 3 dB is different. It is the same for the modules 1B and 2H (fig. 2).

Now that the geometry of the module is known the computation of each component scattering matrix can be done.

#### 1.2.1 - 3 dB coupler

If the losses are neglected, and if the coupling and the directivity are supposed to be perfect, the scattering matrix for the 3 dB coupler of the mode TE<sub>10</sub> is given by :

$$\sqrt{2}/2 \begin{bmatrix} 0 & 1 & -j & 0 \\ 1 & 0 & 0 & -j \\ -j & 0 & 0 & 1 \\ 0 & -j & 1 & 0 \end{bmatrix}$$



This matrix links the electric field of all the waves which are going into to the ones which are going out of the 3 dB coupler, therefore  $Er_1, Er_4, Ei_2, Ei_3$  to  $Ei_1, Ei_4, Er_2, Er_3$  (i and r stand for the incident and reflected waves).

From the previous matrix, the reduced matrix  $\vec{T}$  which is a transmission matrix can be written :

$$\vec{T} = \sqrt{2}/2 \begin{bmatrix} 1 & -j \\ -j & 1 \end{bmatrix}$$

The 4 ports are labeled 1 to 4. The incident and the reflected fields are noted  $Ei_{1 \rightarrow 4}$  and  $Er_{1 \rightarrow 4}$  for the 4 ports and  $\phi$  is the value of the phase shifter put in the output port n° 3 in order to adjust the 2 output incident phase shifts to  $0^\circ$ . And the reflexion coefficients at the output are labeled  $\rho_2, \rho_3, \rho_4$ . From this, one can write :

$$Er_{2 \rightarrow 4} = \rho_{2 \rightarrow 4} Ei_{2 \rightarrow 4}$$

Where the port 1 is the input port, the port 4 is the balance port of the hybrid junction. There, a short-circuit or a load can be put. The ports 2 and 3 are the output ports.

From the previous definition the following matrixes can be defined :

$$\vec{\rho} = \begin{bmatrix} \rho_2 & 0 \\ 0 & \rho_3 \end{bmatrix} \text{ and } \vec{F} = \begin{bmatrix} 1 & 0 \\ 0 & e^{i\phi} \end{bmatrix}$$

The first one is the reflexion matrix at the output ports of the hybrid coupler and the second one is the transmission matrix which takes into account the p. s..

Then with the knowledge of the these matrixes and by using the relations which link the different components of the electric field, the matrix M can be defined as (see annexe 1) :

$$\vec{M} = \vec{T} \cdot \vec{F} \cdot \vec{\rho} \cdot \vec{F} \cdot \vec{T}$$

The different components of the electric field are then given by the following relations :

$$\begin{bmatrix} Er_1 \\ \rho_4 Ei_4 \end{bmatrix} = \vec{M} \begin{bmatrix} Ei_1 \\ Ei_4 \end{bmatrix} \quad and \quad \begin{bmatrix} Ei_2 \\ Ei_3 \end{bmatrix} = \vec{T} \begin{bmatrix} Ei_1 \\ Ei_4 \end{bmatrix}$$

From this computation it appears that a wave coming from port 1 sees its phase changing of  $-90^\circ$  on port 3 compare to  $0^\circ$  on port 2. The behavior at the input port mainly depends on what is set on the hybrid balance port and on the reflexion coefficients.

When the electric length and the matching impedance are the same for the 2 output ports 2 and 3 the whole reflected power is going into port 4 (fig. 3). Therefore if there is a load, the total reflected power will be absorbed and the input port sees a very low reflexion coefficient. If the phase or the amplitude of the reflexion coefficients are slightly different, the input reflexion power remains low. It is like an equilibrium state. On the contrary if there is a short circuit, the reflected power is circulating once more. And depending on the output conditions, a resonance can occur.

If a 90° p.s. is added on port 3 to do in such a way that the incident phase is the same for the 2 output ports, for the same condition the reflected power is going into port 1. Therefore if there is a short circuit on port 4, it will see no power. But this argument is true only in one case. That is when all the right conditions are respected. If they are not, for example due to the value of the p.s., or due to the reflexion coefficient phases which have a difference of 1°, the short circuit will see power. This state is an unstable state.

If the value of the phase shifter is slightly different from 90°, or if the phase of the reflexion coefficient of the 2 output ports is slightly different, a resonance occurs (fig. 4). This underlines the difficulty of putting a short circuit on the 3 dB balance port.

#### 1.2.2 - Phase shifter

The aim of such a device is to change the electric length of a waveguide by putting a discontinuity. This can be done by a capacitive thin window, or by stubs. But due to the high electric field encountered inside the waveguide it seems safer to use step transformer phase shifter.

The electric length  $Le$  of a waveguide is given by :

$$Le = 2\pi l / \lambda g$$

With  $l$  the length of the waveguide and  $\lambda g$  the wavelength which is related to the vacuum wavelength  $\lambda$  and to the larger size of the waveguide  $a$  by :

$$\lambda_g = \lambda / \sqrt{1 - (\lambda/2a)^2}$$

for the mode TE<sub>10</sub>.

If the size  $a$  is decreased the electric length is decreased and the phase velocity is increased. It means that the phase at the output of a straight waveguide will be late compared to the one of a waveguide with a p.s. . To match this change of size, quarter wavelength step transformers are used. The phase shift between the two lines is then given by :

$$\Delta = 2\pi l(1/\lambda_{g1} - 1/\lambda_{g2})$$

Where the change in the computation of the waveguide wavelength is that  $a$  is replaced by  $a_1$  and  $a_2$ .

## 2 - THEORETICAL COMPUTATION OF THE ANTENNA'S SCATTERING MATRIX

### 2.1 - Definition and properties of the Scattering Matrix (S.M)

#### 2.1.1 - Definition

Considering an electric multipolar device (E) the scattering matrix  $S$  is the matrix which links the electric field of the wave going out of (E)  $b_i$  to the electric field of the wave going into (E)  $a_i$ . This can be written for one mode only or for many modes as :

$$\overline{b_i} = \overline{S a_i}$$

With 1 to N and N the number of ports of the multipole (E).

The parameters  $S_{ij}$  are complex. In next chapter  $|S_{ij}|$  will be its modulus and  $\angle S_{ij}$  its phase.

### 2.1.2 - Properties

The main properties of these parameters are that :

The output and input powers are proportionnal to  $b_i.b_i^*$  and  $a_i.a_i^*$ .

The matrix is symmetric :  $S_{ij} = S_{ji}$ .

The equality of the input to the output power implies that :

$$S_{ij}.S_{jk}^* = \delta_{ij} \qquad \delta_{ij} = 1 \text{ for } i = j$$

$$\qquad \qquad \qquad \delta_{ij} = 0 \text{ for } i \neq j$$

(when an index is twice there is summation on it).

### 2.1.3 - Size of the matrix

For the case of one module there are 10 ports. Therefore the dimension of the S.M. is 10 x 10. On the 4th port of the hybrid junction a short-circuit or a load can be set then the matrix size becomes 9 x 9. For the whole antenna which is made of 16 modules its size is 144 x 144.

## 2.2 - Computation of a half a module S.M.

### Notation :

E is taken to design the electric field. the indexes i and r mean the incident and the reflected waves. The number following these indexes are shown on (fig. 5). The matrixes of the 90° and of the 180° multijunctions are given by the code SWAN (Slow Wave ANTenna) from MOREAU NGUYEN [3]. In this code only one dimension is taken into account to calculate the matrix of the discontinuity. There the waveguide is supposed to be infinite in the  $\alpha$  dimension. The higher modes are taken into account.

In the following computation, only the TE<sub>10</sub> is considered. And the losses are neglected. For the main components of the module, the following hypothesis are taken : the phase shifters are represented only by there phase value and the real geometry of the phase shifter is supposed to be perfect, the 3 dB coupler is supposed to be ideal.

For the following computation the notation will be as described next :

A vector  $V$  is written as  $\overline{V}$  when it is written on one line and  $\overline{T}$  when it is written on one column.

A matrix M is written as  $\overline{M}$ .

Every matrix  $\overline{M}$  can be written as :



$$\bar{M} = \begin{bmatrix} M^{00} & \bar{T} \\ \bar{T} & \bar{C} \end{bmatrix}$$

The term  $M^{00}$  is representing the VSWR of the input port for example for the  $90^\circ$  multijunction.

The vector  $\bar{T}$  gives the transmission factor between the input port and the output ports. For the  $90^\circ$  multijunction the amplitude of each component of  $T$  is  $\sqrt{2}/2$ . That means that the input power is divided into 2. The phases of these components are respectively  $0^\circ$  and  $90^\circ$ .

The components of the matrix  $\bar{C}$  are the coupling coefficients between the neighbouring waveguides through the considered discontinuity.

For the following :

The matrix of the  $90^\circ$  and of the  $180^\circ$  multijunctions will be noted  $S_6$  and  $S_4$ . The matrix  $I$  is the matrix unity of dimensions  $2 \times 2$  and the matrix  $S_{11}$  is the matrix of half a module.

$\Phi_3, \Phi_5, \Phi_7$  are the electric lengths of :

- the distance between the 3 dB coupler and the  $180^\circ$  discontinuity,
- the length of the  $180^\circ$  multijunction,
- the length of the  $90^\circ$  multijunction.

In the annexe 2 it is shown that the matrix of half a module  $\bar{S}_{11}$  can be written as :

$$S_{11}^{00} = e^{-j\phi_3} \left\{ E^{-j\phi_3} S_4^{00} + \bar{T}_4 e^{-j\phi_5} \begin{bmatrix} S_6^{00} & 0 \\ 0 & S_6^{00} \end{bmatrix} \left( \bar{1} - \bar{C}_4 e^{-j\phi_5} \begin{bmatrix} S_6^{00} & 0 \\ 0 & S_6^{00} \end{bmatrix} \right)^{-1} \times e^{-j\phi_5} \bar{T}_4 e^{-j\phi_3} \right\}$$

$$\begin{aligned} \bar{T}_{11} &= \bar{T}_4 e^{-j(\phi_3 + \phi_5)} \left\{ \begin{bmatrix} S_6^{00} & 0 \\ 0 & S_6^{00} \end{bmatrix} \left( \bar{1} - \bar{C}_4 e^{-j2\phi_5} \begin{bmatrix} S_6^{00} & 0 \\ 0 & S_6^{00} \end{bmatrix} \right)^{-1} e^{-j2\phi_5} \bar{C}_4 \right. \\ &\quad \left. \times \begin{bmatrix} \bar{T}_6 & 00 \\ 00 & \bar{T}_6 \end{bmatrix} e^{-j\phi_7} + \begin{bmatrix} \bar{T}_6 & 00 \\ 00 & \bar{T}_6 \end{bmatrix} e^{-j\phi_7} \right\} \end{aligned}$$

$$\bar{T}_{11} = e^{-j\phi_7} \begin{bmatrix} \bar{T}_6 & 0 \\ 0 & \bar{T}_6 \end{bmatrix} \left( \bar{1} - \bar{C}_4 e^{-j\phi_5} \begin{bmatrix} S_6^{00} & 0 \\ 0 & S_6^{00} \end{bmatrix} \right)^{-1} e^{-j\phi_5} \bar{T}_4 e^{-j\phi_3}$$

$$\begin{aligned} \bar{C}_{11} &= e^{-j\phi_7} \begin{bmatrix} \bar{T}_6 & 0 \\ 0 & \bar{T}_6 \end{bmatrix} \left( \bar{1} - \bar{C}_4 e^{-j2\phi_5} \begin{bmatrix} S_6^{00} & 0 \\ 0 & S_6^{00} \end{bmatrix} \right)^{-1} e^{-j2\phi_5} \bar{C}_4 \\ &\quad \times \begin{bmatrix} \bar{T}_6 & 00 \\ 00 & \bar{T}_6 \end{bmatrix} e^{-j\phi_7} + \begin{bmatrix} \bar{C}_6 & 00 \\ 00 & \bar{C}_6 \end{bmatrix} e^{-2j\phi_7} \end{aligned}$$

### 2.3 - Computation of a module S.M.

The computation of the whole matrix must take into account the 2 half module matrixes and the matrix of the 3 dB coupler.

For the matrix of the other half module, the computation is almost the same than before, the only changes are  $\phi_3 \rightarrow \phi_8$  and  $\phi_7 \rightarrow \phi_9$ . Therefore it leads to 2 matrixes  $\bar{S}_{11}$  and  $\bar{S}_{12}$  of dimensions 9 x 9.

For the 3 dB coupler, the following transmission matrix is considered with the same hypothesis than in chapter 1.2.1.

$$\bar{T}_2 = \sqrt{2/2} \begin{bmatrix} -j & 1 \\ 1 & -j \end{bmatrix}$$

In the annexe 3 the computation of the matrix  $\bar{M}$  of the whole module is given. The result is as following :

$$\bar{M} = \begin{bmatrix} \bar{T}_2 \begin{bmatrix} S_{11}^{00} & 0 \\ 0 & S_2^{00} \end{bmatrix} \bar{T}_2 & \bar{T}_{12} \begin{bmatrix} \bar{T}_{11} & 0000 \\ 0000 & \bar{T}_2 \end{bmatrix} \\ \begin{bmatrix} 0 \\ \bar{T}_{11} \\ 0 \\ 0 \\ 0 \\ 0 \end{bmatrix} & \begin{bmatrix} 0 \\ 0 \\ 0 \\ 0 \\ \bar{T}_{12} \\ 0 \end{bmatrix} \begin{bmatrix} \bar{C}_{11} & \bar{0} \\ \bar{0} & \bar{C}_{12} \end{bmatrix} \end{bmatrix}$$

In this expression one can see easily that, as expected, the matrix is symmetric.

The matrix  $\bar{0}$  is the matrix null of dimension 4 x 4.

If now a load or a short-circuit is added on the 3 dB balance port which can be represented as a reflexion coefficient  $\rho_5$  which links  $Ei_5$  and  $Er_5$  as :

$$Ei_5 = \rho_5 Er_5$$

And if the matrix  $\bar{M}$  is written as :

$$\bar{M} = \begin{bmatrix} M^{00} & M^{01} & \bar{M} \\ M^{10} & M^{11} & \bar{M}' \\ \bar{M} & \bar{M}' & \bar{C} \end{bmatrix}$$

Where :  $M^{00}$  and  $M^{11}$  are the reflexion coefficients of the module seen at the input port or at the 3 dB coupler balance port, when all the ports have been matched.

The term  $M^{01}$  gives the hybrid junction directivity. The vector  $\bar{M}$  and  $\bar{M}'$  give the transmission coefficients between the input port or the 3dB coupler balance port and the 8 output ports.

The matrix  $\bar{N}$  of dimension 9 x 9 is given as :

$$\bar{N} = \begin{bmatrix} M^{00} + \frac{M^{01} M^{10}}{\Delta} \rho_5 & \frac{M^{01} \rho_5 \bar{M}'}{\Delta} + \bar{M} \\ \bar{M} + \frac{\bar{M}' \rho_5 M^{10}}{\Delta} & \frac{\bar{M}' \rho_5 \bar{M}'}{\Delta} + C \end{bmatrix}$$

With  $\Delta = 1 - \rho_5 M^{11}$

If a very good load is put on port 5, this implies :

$$\rho_5 = 0$$

For this case the expression of  $\bar{N}$  is easier :

$$\bar{N} = \begin{bmatrix} M^{00} & \bar{M} \\ \bar{M} & \bar{C} \end{bmatrix}$$

Thus the matrix  $\bar{N}$  is the same than the matrix  $\bar{M}$  where the term  $M^{00}$  and the vector  $\bar{M}$  and its transposed vector have been removed when the load put on the 3 dB balance port is good. It means also that the knowledge of the module 10 x 10 matrix is sufficient to determine the 9 x 9 matrix of the same module when a perfect load is set on the 3 dB balance port just by cancelling the line and the column belonging to this port.

#### 2.3.1 - Remarks

For the matrix  $\bar{M}$  the different parameters have the following meanings :

- $M_{00}$  and  $M_{11}$  give the VSWR of the matched module seen from the 2 input ports 1 and 5,
- $M_{01}$  gives the directivity of the 3 dB coupler,
- $M_{0i}$  and  $M_{1i}$  for  $i = 2$  to 9 give the transmission factor. This one is necessary corresponding to a power transmission of 1/8 th (if the 3 dB directivity is perfect),
- $M_{ii}$  for  $i = 2$  to 9 gives to the VSWR of the matched module seen from one output waveguide,
- $M_{ij}$  for  $i \neq j$  and  $i$  and  $j$  different from 0 and 1 gives the coupling between 2 output waveguides.

For matrix  $\bar{N}$  :

-  $N_{00}, N_{0i}, N_{ii}, N_{ij}, i \neq j (i, j = 1 \text{ to } 8)$  have the same meanings than  $M_{00}, M_{0l}, M_{lm}, l \neq m (l, m = 2 \text{ to } 9)$ ,

-  $N_{ij}$  for  $j = i + 4$  gives the directivity.

#### 2.4 - The antenna SM

When the matrix  $\bar{S}_i$  of every module  $i$  is known, one can write the matrix of one coupler. In fact there are 4 different families of module. But really every module is different from the other. This is due to the fact that the position of the short-circuit put on the 3 dB coupler balance port is different for every module. Then the scattering matrix of one coupler can be written as :

$$\begin{bmatrix} \bar{S}_1 & & 0 \\ & \bar{S}_2 & \\ 0 & & \bar{S}_{16} \end{bmatrix}$$

#### 2.5 - Results

##### 2.5.1 - Module prototype

##### 2.5.1.1 - With a load

(tab. 1).

The different properties described in chapter 2.1.2 are found. But due to the symmetries of the prototypes some other properties appear for the matrix  $\bar{N}$  :

$$- |N_{0i}| = |N_{01}| = \sqrt{1}/8 \text{ for } i = 1 \text{ to } 8.$$

-  $\angle N_{0i} = \angle N_{0i-1} + 90^\circ$  for  $i = 2$  to  $4$  and  $i = 6$  to  $8$ . This is due to the phase shifter set in each neighbouring output waveguide to generate the N// spectra.

$$- |N_{ii}| = |N_{11}| \text{ for } i = 1 \text{ to } 8.$$

-  $\angle N_{ii} = \angle N_{11} + (j-1) \times 180^\circ$ . The  $90^\circ$  p.s. is seen twice by the wave, first by the incident wave, then by the reflected wave.

-  $|N_{13}| = |N_{14}|$  and  $\angle N_{14} = \angle N_{13} + 90^\circ$ . These parameters give the coupling through the  $180^\circ$  multijunction discontinuity.

-  $|N_{ij}| = |N_{15}|$   $i = 1$  to  $4$ ,  $i = 5$  to  $8$ . This gives the coupling through the 3 dB coupler. It equals to 0 if the load and the 3 dB coupler are supposed perfect.

$$- \angle N_{ij+1} = \angle N_{ij} + 90^\circ.$$

- If the  $9 \times 9$  S.M. is reduced to a  $8 \times 8$  matrix by removing line and column 0, the new obtained matrix is symmetric compared to its 2nd diagonal.

- Due to all these properties the knowing of the 6 parameters  $N_{00}, N_{01}, N_{11}, N_{12}, N_{13}, N_{15}$  is sufficient to find the 81 parameters of the matrix N.

- For the line or the column 1 to 8 the output is less than the input. The reason is that 1/8 th of the power is lost into the load.

#### 2.5.1.2 - With a short-circuit

(tab. 2)

These same properties than before are observed excepted :

- The input is equal to the output for every line and column.

- The amplitude of the  $N_{15}$  parameter is different from 0. That means that the short-circuit is playing a role. But if the values of the reflexion coefficient are the same for the 2 rows of 4 waveguides the input port will get the total reflected power.

- If the short-circuit is moved the only parameters which are not moving are :  $N_{00}$  and  $N_{01}$ .

When the matrix of one module is known, one can compute the reflected power at the input of the module.

First we can define :

$$\rho = \begin{bmatrix} \rho_2 & & & \\ & \rho_3 & & 0 \\ & & \cdot & \\ 0 & & & \cdot \\ & & & \rho_9 \end{bmatrix}$$

as the matrix which gives the reflexion coefficient on each output waveguide.



As before the matrix (9 x 9) of the module is called  $\bar{N}$ . The reflexion coefficient at the input port  $\rho_1$  is then given by :

$$\rho_1 = N^{11} + \bar{T} \rho \left\{ \bar{1} - \bar{C} \rho \right\}^{-1} \bar{T}$$

With  $\bar{1}$  the matrix unity of dimension 8 x 8.

That means  $\rho_1$  is the addition of the module input port reflexion coefficient to the output ports coefficient reflexion effect.

The total electric field at the end of each output waveguide is then given by :

$$\overline{Et + Er} = \left\{ \bar{1} + \bar{\rho} \right\} \left\{ \bar{1} - \bar{C} \rho \right\}^{-1} \bar{T} Et_1$$

With  $Et_1$  the electric field at the input.

The computation of the reflexion at the input has been done for the prototype with the hypothesis of an identical reflexion coefficient on every output waveguide. This has been done for 2 cases : with a load or with a short-circuit on the 3 dB balance port. The amplitude has been noted  $\rho$  and the phase  $\theta$ . One can see on fig. 6 that if the amplitude of the reflexion coefficient at the output is  $\rho$  the reflexion coefficient at the input is decreased to better than  $\rho^2$ . And the behavior is slightly better with a load than with a short-circuit. For the case with a short-circuit the computation has been performed for the ideal conditions.

2.5.2 - Module 02.5.2.1 - 10 x 10 matrix

(tab. 3 and 4)

For this module the 10 x 10 matrix  $\bar{M}$  has been computed. Some more properties have been seen :

If the matrix  $\bar{M}$  is replaced by the matrix  $\bar{M}'$  which is defined by :

$$- M'_{0i} = M_{0i+1} \text{ for } i = 1 \text{ to } 7.$$

$$- M'_{00} = M_{00}.$$

$$- M'_{ij} = M_{i+1j+1} \text{ for } i = 1 \text{ to } 7.$$

$$- M'_{09} = M_{01}.$$

$$- M'_{9i} = M_{1i+1} \text{ for } i = 1 \text{ to } 7.$$

$$- M'_{99} = M_{11}.$$

$$M'_{ij} = M'_{ji}.$$

That means that matrix  $\bar{M}'$  is almost the same matrix than  $\bar{M}$ , the only change is that line and column 1 have been moved to line and column 9. The other line and column have been moved to complete.

It can be observed that :

- The reduced matrix  $\bar{M}$  which is the matrix  $\bar{M}'$  minus line and column 9 has the same properties than matrix  $\bar{N}$  for the module with a load on the 4 th balance port. Therefore what has been seen theoretically is verified.

-  $M'_{99} = M'_{00}$ . The SWR of the matched antenna is the same seen by the 2 input ports.

-  $M'_{9i} = M'_{0i} = \sqrt{1/8}$  for  $i = 1$  to 8.

- The only new parameter is  $M'_{09}$ . Therefore to determine the 10 x 10 matrix the knowing of 7 parameters is necessary. These parameters are  $M'_{00}, M'_{01}, M'_{11}, M'_{12}, M'_{13}, M'_{15}, M'_{09}$ .

### 2.5.3 - The antenna scattering matrix

First there is to determine the 10 x 10 matrix of the 4 different modules  $M'(1H), M'(1B), M'(2H), M'(2B)$  (tab. 3, 5, 6).

The modulus of the parameters of these matrixes are the same than for module 0. For the phase it is different. That is mainly due to the fact that the phase shifter + 45° or + 135° which is put to compensate the 90° phase shift of the 3 dB coupler and the poloidal shape is just between the 3 dB coupler and the 180° multijunction (fig. 2). Therefore for the phase the matrix  $M'$  is dissymmetric.

The main difference is that the reduced matrix  $8 \times 8 \bar{P}$  obtained when the lines and the columns 0 and 9 are canceled is no more symmetric. But all the other relations are still true. The reduced matrix  $\bar{P}(1H)$  and  $\bar{P}(1B)$  are equal to respectively  $\bar{P}(2H)$  and  $\bar{P}(2B)$ . The main difference between the 2 kinds is that one kind is the symmetric of the other compared to the 2 nd diagonal.

But in the antenna the input port of a 1H or 2B module type is respectively port 1 and 5. It is the same for module 1B and 2H. Therefore the behavior of module 1H (resp. 1B) is the same than module 2B (resp. 2H). On the antenna the short-circuit has not been put at the same place for all modules. But the matrix of modules of the same type are slightly different.

To obtained the matrix  $9 \times 9$  of each module the position of the short circuit has been taken into account. For each module this position is different in order to be far from a resonance. This difference can be explained by geometric imperfection. The matrix for the module 1H and 1B are given in tab. 7, 8. One can see that the amplitudes of the S parameters are highly changed and that they depend on the module. A few examples are given in the following tabula :

	Module 1H	Module 1B	Matrix 9 X 9 with a load
$ N_{11} $	0.391	0.612	0.5
$ N_{12} $	0.639	0.612	0.62
$ N_{13} $	0.347	0.206	0.25
$ N_{15} $	0.126	0.121	0.

One can also observe that from the phase point of view the matrix is no more symmetric compared to the second diagonal of the reduced matrix obtained by canceling the first line and the first column. The transmission factor and the global standing wave ratio seem to be unchanged.

### 3 - EXPERIMENTAL MEASUREMENT OF A MODULE S.M.

#### 3.1 - Measurement method

To obtain the parameter  $S_{ij}$  of the scattering matrix of a module, the waveguide  $j$  must be excited and all the others matched with good loads ( $VSWR < 1.05$ ). By this way the powers and the phases  $P_i$ ,  $P_j$ ,  $\phi_i$  and  $\phi_j$  are measured. The parameter  $S_{ij}$  is deduced following the given relation :

$$- |S_{ij}| = \sqrt{(P_i/P_j)},$$

$$- \angle S_{ij} = \phi_i - \phi_j.$$

therefore to realize the measurement the main components which are needed are :

- A coaxial waveguide adaptator to excite the input waveguide. It can be used for only the ports which have standard sizes. In fact for the module input the sizes are 76 x 34 (mm x mm). A little higher than the WR 284 waveguide. Thus a linear taper has been used to adjust the 2 sizes. For the output waveguides this can't be used.

The sizes are 76 x 6.75 or 8 mm and it is difficult to realize a taper which can be in good contact with the wall between the small output waveguide which has a thickness of 2 mm. Therefore a new technic has been used which will be explained further.

Load with good VSWR. The problem is the same than for the previous item. Therefore carbon cone type load set on a short-circuit which sizes are the output waveguides ones has been developped.

Bidirectional couplers for the measurement of the phase and the amplitude of the incident and the reflected waves. The same remark can be done. For the smaller size waveguide a coupler has been developped.

All the measurements have been performed by using a Hewlett Packard network analyser.

### 3.1.1 - Exciting magnetic probe

(Fig. 7) Photo n° 3

To excite non standard waveguides it has been decided to realize a magnetic loop, the end of the loop is on a short-circuit. Its surface is of  $\lambda_g/4 \times 4mm^2$  and is set in the E plane. Once the probe is put inside the waveguide the VSWR seen by the generator is not good. Therefore it has been improved by putting a  $50\Omega$  load at the end of the loop. The loop is set perpendicularly to a short-circuit which can enter inside the smaller waveguides. The good contact between the waveguide and the short-circuit is obtained by using Beryllium copper spring. Finally the coupling and the VSWR are 2.5 dB and 1.38.

### 3.1.2 - Smaller size waveguide coupler

(fig. 7) Photo n° 4

Due to the geometry of the module the measurement of the electric field has to be done on the smaller waveguide size. Therefore the designed coupler has to use magnetic loops. To reach a good directivity 2 loops distant from  $\lambda g/4$  are set on the waveguide. Then they are linked to a coaxial 3 dB coupler. A variable phase shifter and a variable attenuator are used to adjust electric length of the coaxial wires and of the loop from one to the other. The coupling of such a coupler is around 30 dB and its directivity around 25 dB.

Looking at (fig. 7) it appears that probe 1 measures the incident wave with a phase  $\Phi$  and probe 2 with  $\Phi - 90^\circ$ . Therefore :

- Half of the power from probe 1 goes to port 3 with a phase  $\Phi$  .

- Half of the power from probe 2 goes to port 3 with a phase  $\Phi - 180^\circ$ .

- Half of the power from probe 1 goes to port 4 with a phase  $\Phi - 90^\circ$ .

- Half of the power from probe 2 goes to port 4 with a phase  $\Phi - 90^\circ$ .

Thus on port 4 only the incident wave is seen. It can be shown the same way that the reflected wave is seen by port 3.

The probes are set at 138 mm from the module mouth. Thus after the measurement, corrections must be done to have the true S parameters for the module beginning at the vacuum window till the module mouth.

### 3.1.3 - Accuracy

The accuracy is mainly function of the VSWR of the load and of the directivity of the directional coupler. For the first the VSWR is better than 1.08. For the second the directivity D is 24.9 dB. Noting  $\alpha$  the ratio of the amplitude of the electric field of the opposing wave to the one of the measured wave, for the amplitude the relative error is given by :

$$\Delta E/E \approx \alpha \cdot 10^{(D/20)}$$

And for the phase by :

$$\Delta \Psi = \text{arctg}(\alpha \cdot 10^{(D/20)})$$

By applying these relations to the case of the measurement it appears that :

- $\Delta|S|/|S|$  is generally less than 4 %,
- $\Delta \angle S < 3^\circ$ .

If the results of the measurement are taken into account and if the equality of the S parameters described in chapter 2.1.2 is supposed. By taking into account the mean value and the discrepancy the results are that :

- $\Delta|S|/|S| < 18\%$ ,
- $\Delta \angle S < 20^\circ$ .



This have been done for the module prototype. For the other measurements the discrepancy has been reduced to less than 10 % for the amplitude and around  $10^\circ$  for the phase.

### 3.2 - Results

#### 3.2.1 - 9 x 9 S.M. of the prototype

##### 3.2.1.1 - With a load

(tab. 9)

For the prototype the measurement has been done for the module with its RF window. The results are following.

The general properties defined in chapter 2.5.1.1 are verified :

- The power conservation is find  $0.877 \pm 0.09$ . This is less than 1, because 1/8 th of the total power is going into the load.

- The matrix is symmetric.

On the tab. 7 one can find the main S parameters :

$N_{00}$  which gives the reflexion of the module at the input. The value is corresponding to a VSWR of 1.18. This value is mainly due to the thickness of the inside walls.

The directivity of the 3 dB coupler given by the parameter  $N_{15}$  is of the order of 17 to 20 dB.

The transmission factor between the input port and the output ports  $N_{01}$  is not far from  $\sqrt{1/8}(0.354)$

The reflexion coefficient of the module seen at each output waveguide is high. The value for the  $N_{11}$  parameter is 0.498. One must remember that the theoretical one is 0.504.

The coupling through the  $90^\circ$  multijunction is  $N_{12}$  equal to 0.63, and through the  $180^\circ$  multijunction it is  $N_{13}$  equal to 0.277. The theoretical values are respectively 0.612 and 0.247.

One can also see that the different relations of phase are verified.

If the short-circuit is put on one output waveguide, for the simulation of a multipactor breakdown, the S parameters of the neighbouring waveguides are changed. For example if a short-circuit is put in the port 6 (0 is the input port) the only parameters which are changing are :  $N_{65}, N_{75}, N_{85}$ . The more astonishing result of this experience is that the reflexion coefficient at the module input is unchanged, therefore it means that a breakdown can occur inside a small waveguide without to be seen at the input port. That can be very dangerous for continuous wave due to the thermal heating by an RF plasma.

Parameter	With a short-circuit on the output port 6	without
$N_{65}$	0.51	0.67
$N_{75}$	0.35	0.24
$N_{85}$	0.34	0.24

### 3.2.1.2 - With a short-circuit

(Tab. 10)

Compared to the previous chapter only one parameter is highly changed  $N_{15}$  which is increased from 0.015 to 0.11. That means that the short-circuit has an effect on the reflected power, it increases the coupling between the waveguide from one level to the other by a factor 10.

The general properties of the scattering matrix are verified : the power conservation is also found  $0.99 \pm 0.127$  and the matrix is symmetric.

The effect of moving the short-circuit on the 6 main parameters has been observed. It has been shown that only  $N_{00}, N_{01}$  stay unchanged. The amplitude of  $N_{15}$  does not move too much. But for the others it is very important :  $N_{12}, N_{13}, N_{23}$  (fig. 8 and 9).

### 3.2.2 - 10 x 10 S.M. of the module 0

(Tab. 11 and 12)

For the measurements of the module 0 and of the modules of serie only the copper part of the module has been taken into account. The measurements have been performed using the same method than previously. It leads to the following results.

The matrix  $M'$  has been considered in these tables. One can see that the coefficients of transmission from port 0 to 1 and from port 10 to 1 are the same. This is due to the fact that the behavior of the module is the same seen by port 0 or by port 10 which are in fact the 2 input ports of the 3 dB coupler.

One can see that the seven S parameters necessary to define the module have an experimental value very close to the experimental one.

S parameter	Theoretical amplitude	Experimental amplitude	Theoretical phase	Experimental phase
$M'_{00}$	0.03	0.03	116	177
$M'_{01}$	0.35	0.37	- 137	- 145
$M'_{11}$	0.5	0.44	139	140
$M'_{12}$	0.62	0.63	- 4	3
$M'_{13}$	0.25	0.29	- 144	- 129
$M'_{15}$	0	$\approx 0.01$		
$M'_{09}$	$< 10^{-5}$	0.05	6	- 13

Now that the matrixes of the antennae are obtained one can see what can be done with.

#### 4 - USE OF THE S.M.

##### 4.1 - Observation of the behavior of the antenna in front of the plasma

On some module, RF probes will be set near the plasma to measure the total electric field  $V_i' + V_i'' = V_t i$  ( $i \rightarrow 1, 8$ ) for each output port. The incident and the reflected electric fields measurement of each module's input port is also done. Therefore it gives the incident and the reflected fields  $V'_0$  and  $V''_0$  (0 is for the input port and 1 to 8 are for the output ports). As seen previously the knowing of the scattering matrix gives the relation :

$$\vec{V}'' = \dot{N} \vec{V}'$$

Which can be written as :

$$\vec{V}'' = \begin{bmatrix} N_{00} & \vec{T} \\ \vec{T} & \dot{C} \end{bmatrix} \vec{V}'$$

Therefore the reflected electric fields on each output waveguide are given by :

$$\vec{V}'_{1 \rightarrow 8} = (\dot{I}_8 x_8 + \dot{C})^{-1} (\vec{V}_t - \vec{T} V'_0)$$

And the incident electric fields are given by :

$$\vec{V}''_{1 \rightarrow 8} = \vec{V}_t - \vec{V}'_{1 \rightarrow 8}$$

Then the incident and the reflected fields for each output port are known. And the behavior of the antenna can be observed. The incident wave and the reflected wave electric values obtained experimentally will be compared to the theoretical ones given by a computation using the plasma admittance matrix given by the code SWAN and the antenna scattering matrix. This will be done to see for example if breakdowns are occurring under vacuum due to multipactor.

#### 4.2 - Computation of the coupling coefficients and the real N// spectra

When the antennas are in front of the plasma, the main part of the power is going into the plasma and the other is going back into the waveguides. For one part the power reflected of the waveguide  $i$  is coming from the same waveguide but for the other part it can come from other neighbouring waveguides  $j$ . The coupling can be defined as a S parameter. In fact for  $N$  waveguides the plasma is like a  $N$  poles. The power is going into and out.

The code SWAN from MOREAU-NGUYEN gives for the 32 horizontal waveguides of one antenna the matrix admittance  $P_0$  of the plasma. The electronic density and its gradient at the mouth of the antenna must be known. The measurement of these parameters will be given by Langmuir probe set at the antenna mouth.

During the experiment the acquisition gives the input and the output powers and phases of each module. And we can't know what is going on at the antenna mouth. The number of measurements are not sufficient. Therefore the problem of determining the coupling coefficients at the mouth is translated to its determination at the input of each module. Due to the construction of the antenna if one considers only the coupling on the horizontal direction, that means that the coupling in the poloidal direction is neglected, we have to take into account  $2 \times 32$  waveguides. Therefore we must build a plasma matrix  $\bar{P}$  as :

$$\bar{P} = \begin{bmatrix} \bar{M}_{11} & \bar{0} & \bar{M}_{12} & 0 & \dots\dots & \bar{M}_{18} & \bar{0} \\ \bar{0} & \bar{M}_{11} & \bar{0} & \dots & & & \\ \dots\dots\dots & & & & & & \\ \bar{M}_{81} & \dots\dots\dots & & & & & \bar{M}_{88} \end{bmatrix}$$

Build from :

$$\bar{P}_0 = \begin{bmatrix} \bar{M}_{11} & \bar{M}_{12} & \dots\dots\dots & \bar{M}_{18} \\ \cdot & & & \\ \cdot & & & \\ \cdot & & & \\ \cdot & & & \\ \bar{M}_{81} & & & \bar{M}_{88} \end{bmatrix}$$

With the hypothesis that the coupling is neglected in the vertical direction.

The matrix  $\bar{M}_{ij}$  is giving the coupling from the module  $i$  to the module  $j$  through the plasma.

The matrix  $\bar{0}$  is the matrix null with a dimension of 4 x 4.

As said previously one considers only 2 rows of waveguides, it means one row of modules. Therefore the matrix of the half antenna has to be considered :

$$\bar{T} = \begin{bmatrix} \bar{N}_{11} & & & 0 \\ & \bar{N}_{22} & & \\ & & \bar{N}_{33} & \\ 0 & & & \bar{N}_{88} \end{bmatrix}$$

And the incident and the reflected electric fields at each module input must be taken into account  $\bar{V}'_1$  and  $\bar{V}''_1$  which are link together by the relation :

$$\bar{V}''_1 = \bar{T} \bar{V}'_1$$

$$\text{With } \bar{V}'_1 = \begin{array}{c} \left| \begin{array}{l} V'_{11} \\ V'_{12} \\ \cdot \\ V'_{19} \\ \cdot \\ \cdot \end{array} \right| \quad \text{module n}^\circ 1 \end{array}$$

The term  $V'_{11}$  gives the incident electric field at the input of the module 1, the other terms  $V'_{12 \rightarrow 9}$  give it at the outputs of the module 1.



In the annexe 4 it is shown that the reflected fields at the outputs of the modules are given by :

$$\begin{bmatrix} V''_{12 \rightarrow 9} \\ \vdots \\ V''_{82 \rightarrow 9} \end{bmatrix} = \left\{ \begin{bmatrix} \dot{C}_{11} & & \\ & \dot{C}_{22} & \\ & & \ddots \\ & & & \dot{C}_{88} \end{bmatrix} \cdot \begin{bmatrix} \dot{P} \\ \vdots \\ \dot{P} \end{bmatrix} \right\}^{-1} \begin{bmatrix} \bar{T}_{11} & & \\ & \bar{T}_{22} & \\ & & \ddots \\ & & & \bar{T}_{88} \end{bmatrix} \begin{bmatrix} V'_{11} \\ \vdots \\ V'_{81} \end{bmatrix}$$

With here  $\bar{1}$  is the matrix unity of size 64 x 64.

And the reflected field at each module input is given by :

$$\begin{bmatrix} V''_{11} \\ \vdots \\ V''_{81} \end{bmatrix} = \begin{bmatrix} S_{11} & & 0 \\ & S_{21} & \\ & & \ddots \\ 0 & & & S_{81} \end{bmatrix} \begin{bmatrix} V'_{11} \\ \vdots \\ V'_{81} \end{bmatrix} + \begin{bmatrix} \bar{T}_{11} & & 0 \\ & \ddots & \\ & & \bar{T}_{81} \end{bmatrix} \begin{bmatrix} V'_{12 \rightarrow 9} \\ \vdots \\ V'_{82 \rightarrow 9} \end{bmatrix}$$

From the previous relation the conclusion is :

The code SWAN delivers the plasma matrix of scattering. Therefore with the knowing of the antenna matrix of scattering and the knowing of the incident electric field of each module one can compute the reflected field of each module.

This can be then compared to the experimental value. The total electric field at the end of the modules is also known therefore one can compute the real N// injected into the plasma.

If only one module n° i is fed, one can compute the coupling coefficient between each module j and this module i by the relation :

$$V_j/V_i = S(j,i)$$

The determination of the coupling coefficients has been done during the first experiments with the hybrid heating on TORE SUPRA. This work has been done with the help of X. LITAUDON.

The theoretical values have been obtained as said previously. The experimental ones have been given by feeding one klystron only and by measuring the reflected field at the input of each module.

On fig. 10 there is the variation of the amplitude of the  $S(i,i)$  parameters for the modules 6B and 6H depending on the position of the antenna compared to the position of the limiter. The theoretical and the experimental values are given. The hypothesis to calculate the theoretical values are :

- a density at the limiter of  $2 \cdot 10^{12} m^{-3}$ ,
- a density decreasing length of 1.3 cm.

One can see that the shapes are the same for the experimental and the theoretical curves. The experimental values are a little higher than the theoretical ones. If now fig. 11 is observed one can see that for the phase of the  $S(i,i)$  parameters there is a quite large discrepancy. This is done for the module 3 and the module 2. That will be improved in future experiment by increasing the accuracy of the measurements.

The fig. 12 gives the amplitudes of the  $S(i,i)$  parameters for the modules type H and type B for a given position of the antenna. One can observe that the values are higher for the modules at the top. But for the 2 kinds of modules the experimental value is higher than the theoretical one. The theoretical values seem to be independent of the module. For the experimental ones there is like a side effect.

As told previously it was also possible to compare the theoretical and the experimental reflected electric fields when every klystron delivers a power. On fig. 13 the experimental value is between the theoretical value obtained with an electron density at the mouth of the cutoff density or twice the density cutoff. For the phase of the reflected field the agreement between theory and experiment is till now less good (fig. 14).

Finally on fig. 15 there is the experimental spectra due to the low row of modules for one shot on TORE SUPRA where every klystron was fed.

These results are preliminary results. But due to the quite bad conditions of experiment for these first measures one can see that the theoretical and the experimental values are in a quite good agreement. For next experiment on TORE SUPRA these measures will be done with a better accuracy and better experimental working conditions.

## 5 - CONCLUSION

The main property of the multijunction used in TORE SUPRA Lower Hybrid antenna is the self-matching of the output reflexion coefficient. This has been measured and computed. The result is that if the reflexion coefficient is  $\rho$  at the mouth of the multijunction, it becomes  $\rho^2$  at its input. This has been seen also for a module of one antenna with a load or a short-circuit on the 3 dB balance port.

The effect of setting a short-circuit on the 3 dB balance port of the hybrid junction is not too annoying if the module is symmetric and if the reflexion coefficients are low. But this can be dangerous for CW RF wave because it can occur that a breakdown would not be seen at the input. For the modules of serie of the type 1H, 1B, 2H, 2B which are not symmetric, the short-circuit does not play a too important role if the reflexion coefficients at the output are low. If not, it will see approximately half the reflected power.

This study has also proved that there is a quite good agreement between the measurements and the theory for the achievement of the antenna scattering matrix, despite the fact that there have been some problems during the measurement, especially when the amplitude of the S parameters was too low for the determination of the phase with a good accuracy.

The determination of the scattering matrix has allowed us to determine the coupling coefficient of the modules in front of the plasma in a previous experiment of plasma shot of TORE SUPRA. This work will be done one more time to have a better accuracy.

For the next experiments, a few modules have some RF probes from which the behavior of the antenna will be observed.

- [1] G. TONON  
First Lower Hybrid current drive experiments at  
3.7 GHz in TORE SUPRA.  
16 th European conference on controlled fusion  
and plasma physics.
- [2] G. REY  
The 3.7 Ghz Launcher of TORE SUPRA and related  
conditionning results for quasi continuous pulses  
SOFT 88 UTRECHT
- [3] NGUYEN TRONG KHOI  
Couplages d'ondes pour le chauffage des plasmas  
à la fréquence hybride basse.  
Thèse de doctorat (10/02/86)
- [4] D. MOREAU, G. TONON  
Premières expériences de génération de courant  
par injection d'ondes hybrides dans TORE SUPRA.  
Private communication

ANNEXE 1

The matrix of the 3 dB coupler is used to write the relation :

$$\begin{pmatrix} Er_1 \\ Ei_2 \\ Ei_3 \\ Er_4 \end{pmatrix} = \begin{pmatrix} 0 & 1 & -j & 0 \\ 1 & 0 & 0 & -j \\ -j & 0 & 0 & 1 \\ 0 & -j & 1 & 0 \end{pmatrix} \begin{pmatrix} Ei_1 \\ Er_2 \\ Er_3 \\ Ei_4 \end{pmatrix} \frac{\sqrt{2}}{2}$$

$$\begin{pmatrix} Er_1 \\ Er_4 \end{pmatrix} = \frac{\sqrt{2}}{2} \begin{pmatrix} 1 & -j \\ -j & 1 \end{pmatrix} \begin{pmatrix} Er_2 \\ Er_3 \end{pmatrix} = T \begin{pmatrix} Er_2 \\ Er_3 \end{pmatrix}$$

$$\begin{pmatrix} Ei_2 \\ Ei_3 \end{pmatrix} = \frac{\sqrt{2}}{2} \begin{pmatrix} 1 & -j \\ -j & 1 \end{pmatrix} \begin{pmatrix} Ei_1 \\ Ei_4 \end{pmatrix} = T \begin{pmatrix} Ei_1 \\ Ei_4 \end{pmatrix}$$

$$\begin{pmatrix} Ei_3' \\ Er_3 \end{pmatrix} = \begin{pmatrix} e^{j\phi} & 0 \\ 0 & e^{j\phi} \end{pmatrix} \begin{pmatrix} Ei_3 \\ Er_3' \end{pmatrix}$$

$$Ei_2' = Ei_2$$

$$Er_2' = Er_2$$

We want :

$Er_1, Ei_2', Ei_3'$  function of :

$$\begin{pmatrix} Er_2' \\ Er_3' \end{pmatrix} = \begin{pmatrix} \rho_2' & 0 \\ 0 & \rho_3' \end{pmatrix} \begin{pmatrix} Ei_2' \\ Ei_3' \end{pmatrix}$$

$\bar{\rho}$

$$\begin{pmatrix} Er_1 \\ Er_4 \end{pmatrix} = \bar{T} \begin{pmatrix} Er_2 \\ Er_3 \end{pmatrix} = \bar{T} \bar{F} \bar{\rho} \begin{pmatrix} Ei_2' \\ Ei_3' \end{pmatrix}$$



$$\begin{pmatrix} Er_2 \\ Er_3 \end{pmatrix} = \begin{pmatrix} 1 & 0 \\ 0 & e^{j\phi} \end{pmatrix} \begin{pmatrix} Er'_2 \\ Er'_3 \end{pmatrix}$$

$$\begin{pmatrix} Ei'_2 \\ Ei'_3 \end{pmatrix} = \begin{pmatrix} 1 & 0 \\ 0 & e^{j\phi} \end{pmatrix} \begin{pmatrix} Ei_2 \\ Ei_3 \end{pmatrix}$$

$$\bar{F}$$

$$\begin{aligned} \begin{pmatrix} Er_1 \\ Er_4 \end{pmatrix} &= \bar{T} \bar{F} \bar{\rho} \bar{F} \begin{pmatrix} Ei_2 \\ Ei_3 \end{pmatrix} \\ &= \bar{T} \bar{F} \bar{\rho} \bar{F} \bar{T} \begin{pmatrix} Ei_1 \\ Ei_4 \end{pmatrix} \end{aligned}$$

Noting  $Er_4 = \rho_4 Ei_4$

$$\begin{pmatrix} Er_1 \\ \rho_4 Ei_4 \end{pmatrix} = \boxed{\bar{T} \bar{F} \bar{\rho} \bar{F} \bar{T}} \begin{pmatrix} Ei_1 \\ Ei_4 \end{pmatrix}$$

$M$

$$\rho_4 Ei_4 = M_{21} Ei_1 + M_{22} Ei_4$$

$$Ei_4 = \frac{M_{21}}{\rho_4 - M_{22}} Ei_1$$

$$Er_1 = M_{11} Ei_1 + \frac{M_{12} M_{21}}{\rho_4 - M_{22}} Ei_1$$

$$Er_1 = \left( M_{11} + \frac{M_{12} M_{21}}{\rho_4 - M_{22}} \right) Ei_1$$

This gives the reflected electric field at the input port.

$$\begin{pmatrix} Ei_2 \\ Ei_3 \end{pmatrix} = \bar{T} \begin{pmatrix} Ei_1 \\ Ei_4 \end{pmatrix}$$

$$Ei_2 = Ei_1 - jEi_4$$

$$= \left( 1 - \frac{jM_{21}}{\rho_4 - M_{22}} \right) Ei_1$$

$$Ei_3 = \left( -j + \frac{M_{21}}{\rho_4 - M_{22}} \right) Ei_1$$

$$\begin{pmatrix} Ei'_2 \\ Ei'_3 \end{pmatrix} = \bar{F} \begin{pmatrix} Ei_2 \\ Ei_3 \end{pmatrix} = \bar{F} \bar{T} \begin{pmatrix} 1 \\ Ei_4 \end{pmatrix}$$

ANNEXE 2

By taking into account the numerotation given in fig. 5 the different relations at the main planes are :

$$\begin{pmatrix} Er_{24,25,26,27} \\ Ei_{24,25,26,27} \end{pmatrix} = \bar{T}_7 \begin{pmatrix} Er_{16,17,18,19} \\ Ei_{16,17,18,19} \end{pmatrix}$$

$$\begin{pmatrix} Er_{12,13} \\ Ei_{16,18} \\ Ei_{17,19} \end{pmatrix} = \bar{S}_6 \begin{pmatrix} Ei_{12,13} \\ Er_{16,18} \\ Er_{17,19} \end{pmatrix}$$

$$\begin{pmatrix} Er_{12,13} \\ Ei_{12,13} \end{pmatrix} = \bar{T}_5 \begin{pmatrix} Er_{8,9} \\ Ei_{8,9} \end{pmatrix}$$

$$\begin{pmatrix} Er_7 \\ Ei_8 \\ Ei_9 \end{pmatrix} = \bar{S}_4 \begin{pmatrix} Ei_7 \\ Er_8 \\ Er_9 \end{pmatrix}$$

$$\begin{pmatrix} Er_7 \\ Ei_7 \end{pmatrix} = \bar{T}_3 \begin{pmatrix} Er_4 \\ Ei_4 \end{pmatrix}$$

With  $\bar{S}_6$  and  $\bar{S}_4$  the scattering matrixes of the  $90^\circ$  and  $180^\circ$  multijunctions and  $\bar{T}_3, \bar{T}_5, \bar{T}_7$  given by :

$$\bar{T}_i = \begin{pmatrix} e^{j\phi_i} & 0 \\ 0 & e^{-j\phi_i} \end{pmatrix}$$

The S.M. of the lower half module can be called  $\bar{S}_{11}$ .  
Generally  $\bar{S}$  can be written as forward :

$$\bar{S} = \begin{pmatrix} S^{00} & \bar{T} \\ \bar{T} & \bar{C} \end{pmatrix}$$

For example for  $\bar{S}_6$  :

$S_6^{00}$  is the reflexion coefficient of the input port ;  
 $\bar{T}_6$  gives the transmission coefficient and  $\bar{C}$  the coupling  
 between 2 near waveguides and the reflexion coefficient  
 seen from the output waveguides.

The sizes of  $\bar{S}_{11}$  is 5 x 5.  $\bar{S}_{11}$  can be given by :

$$\begin{pmatrix} Er_4 \\ Ei_{24,25,26,27} \end{pmatrix} = \bar{S}_{11} \begin{pmatrix} Ei_4 \\ Er_{24,25,26,27} \end{pmatrix}$$

Or :

$$\begin{aligned} Er_4 &= e^{-j\phi_3} \\ &= e^{-j\phi_3} \left[ S_4^{00} Ei_7 + \bar{T}_4 \begin{pmatrix} Er_8 \\ Er_9 \end{pmatrix} \right] \\ &= e^{-j\phi_3} \left[ S_4^{00} e^{-j\phi_3} Ei_4 + \bar{T}_4 e^{-j\phi_5} \begin{pmatrix} Er_{12} \\ Er_{13} \end{pmatrix} \right] \\ &= e^{-j\phi_3} \left[ S_4^{00} e^{-j\phi_3} Ei_4 + \bar{T}_4 e^{-j\phi_5} \begin{pmatrix} Er_{12} \\ Er_{13} \end{pmatrix} \right] \end{aligned}$$

Or :

$$\begin{aligned} \begin{pmatrix} Er_{12} \\ Er_{13} \end{pmatrix} &= \begin{pmatrix} S_6^{00} & 0 \\ 0 & S_6^{00} \end{pmatrix} \begin{pmatrix} Ei_{12} \\ Ei_{13} \end{pmatrix} + \begin{pmatrix} \bar{T}_6 & 00 \\ 00 & \bar{T}_6 \end{pmatrix} \begin{pmatrix} Er_6 \\ Er_{17} \\ Er_{18} \\ Er_{19} \end{pmatrix} \\ &= \begin{pmatrix} S_6^{00} & 0 \\ 0 & S_6^{00} \end{pmatrix} \begin{pmatrix} Ei_{12} \\ Ei_{13} \end{pmatrix} + \begin{pmatrix} \bar{T}_6 & 00 \\ 00 & \bar{T}_6 \end{pmatrix} e^{-j\phi_7} \begin{pmatrix} Er_{24} \\ Er_{25} \\ Er_{26} \\ Er_{27} \end{pmatrix} \end{aligned}$$

And :

$$\begin{aligned} \begin{pmatrix} Ei_{12} \\ Ei_{13} \end{pmatrix} &= e^{-j\phi_5} \begin{pmatrix} Ei_8 \\ Ei_9 \end{pmatrix} = e^{-j\phi_5} \left[ \bar{T}_4 Ei_7 + \dot{C}_4 \begin{pmatrix} Er_8 \\ Er_9 \end{pmatrix} \right] \\ &= e^{-j\phi_5} \left[ \bar{T}_4 e^{-j\phi_3} Ei_4 + \dot{C}_4 e^{-j\phi_5} \begin{pmatrix} Er_{12} \\ Er_{13} \end{pmatrix} \right] \\ &= e^{-j\phi_5} \left[ \bar{T}_4 e^{-j\phi_3} Ei_4 + \dot{C}_4 e^{-j\phi_5} \left\{ \begin{pmatrix} S_6^{00} & 0 \\ 0 & S_6^{00} \end{pmatrix} \begin{pmatrix} Ei_{12} \\ Ei_{13} \end{pmatrix} + \begin{pmatrix} \bar{T}_6 & 00 \\ 00 & \bar{T}_6 \end{pmatrix} e^{-j\phi_7} \begin{pmatrix} Er_{24} \\ Er_{25} \\ Er_{26} \\ Er_{27} \end{pmatrix} \right\} \right] \end{aligned}$$

Therefore :

$$\begin{pmatrix} Ei_{12} \\ Ei_{13} \end{pmatrix} = \left\{ \begin{matrix} \bar{T}_4 e^{-j\phi_3} \\ 1_{2 \times 2} - e^{-2j\phi_5} \dot{C}_4 \begin{pmatrix} S_6^{00} & 0 \\ 0 & S_6^{00} \end{pmatrix} \end{matrix} \right\}^{-1} e^{-j\phi_5} \left[ \bar{T}_4 e^{-j\phi_3} Ei_4 + \dot{C}_4 e^{-j\phi_5} \begin{pmatrix} \bar{T}_6 & 00 \\ 00 & \bar{T}_6 \end{pmatrix} e^{-j\phi_7} \begin{pmatrix} Er_{24} \\ Er_{25} \\ Er_{26} \\ Er_{27} \end{pmatrix} \right]$$

$$\begin{pmatrix} Er_{12} \\ Er_{13} \end{pmatrix} = \begin{pmatrix} S_6^{00} & 0 \\ 0 & S_6^{00} \end{pmatrix} \left\{ \left[ \bar{I}_{2 \times 2} - e^{-2j\phi_3} \bar{C}_4 \begin{pmatrix} S_6^{00} & 0 \\ 0 & S_6^{00} \end{pmatrix} \right]^{-1} e^{-j\phi_3} \left[ \bar{T}_4 e^{-j\phi_3} Ei_4 + \bar{C}_4 e^{-j\phi_3} \begin{pmatrix} \bar{T}_6 & 00 \\ 00 & \bar{T}_6 \end{pmatrix} e^{-j\phi_7} \begin{pmatrix} Er_{24} \\ Er_{25} \\ Er_{26} \\ Er_{27} \end{pmatrix} \right] \right\} \\ + \begin{pmatrix} \bar{T}_6 & 00 \\ 00 & \bar{T}_6 \end{pmatrix} \begin{pmatrix} Er_{24} \\ Er_{25} \\ Er_{26} \\ Er_{27} \end{pmatrix} e^{-j\phi_7}$$

$$\begin{pmatrix} Er_{12} \\ Er_{13} \end{pmatrix} = \begin{pmatrix} S_6^{00} & 0 \\ 0 & S_6^{00} \end{pmatrix} \left[ \bar{I}_{2 \times 2} - \bar{C}_4 e^{-2j\phi_3} \begin{pmatrix} S_6^{00} & 0 \\ 0 & S_6^{00} \end{pmatrix} \right]^{-1} e^{j\phi_3} T_4 e^{-j\phi_3} Ei_4 \\ + \left\{ \begin{pmatrix} S_6^{00} & 0 \\ 0 & S_6^{00} \end{pmatrix} \left[ \bar{I}_{2 \times 2} - \bar{C}_4 e^{-2j\phi_3} \begin{pmatrix} S_6^{00} & 0 \\ 0 & S_6^{00} \end{pmatrix} \right]^{-1} e^{-2j\phi_3} \bar{C}_4 \begin{pmatrix} \bar{T}_6 & 00 \\ 00 & \bar{T}_6 \end{pmatrix} e^{-j\phi_7} + \begin{pmatrix} \bar{T}_6 & 00 \\ 00 & \bar{T}_6 \end{pmatrix} e^{-j\phi_7} \right\} \begin{pmatrix} Er_{24} \\ Er_{25} \\ Er_{26} \\ Er_{27} \end{pmatrix}$$

Therefore :

$$Er_4 = e^{-j\phi_3} \left\{ S_4^{00} + \bar{T}_4 e^{-j\phi_3} \begin{pmatrix} S_6^{00} & 0 \\ 0 & S_6^{00} \end{pmatrix} \left[ \bar{I}_{2 \times 2} - \bar{C}_4 e^{-2j\phi_3} \begin{pmatrix} S_6^{00} & 0 \\ 0 & S_6^{00} \end{pmatrix} \right]^{-1} e^{-j\phi_3} \bar{T}_4 e^{-j\phi_3} \right\} Ei_4 \\ + \bar{T}_4 e^{-j\phi_3} e^{-j\phi_5} \left\{ \begin{pmatrix} S_6^{00} & 0 \\ 0 & S_6^{00} \end{pmatrix} \left[ \bar{I}_{2 \times 2} - \bar{C}_4 e^{-2j\phi_3} \begin{pmatrix} S_6^{00} & 0 \\ 0 & S_6^{00} \end{pmatrix} \right]^{-1} \right. \\ \left. e^{-j2\phi_3} \bar{C}_4 \begin{pmatrix} \bar{T}_6 & 00 \\ 00 & \bar{T}_6 \end{pmatrix} e^{-j\phi_7} + \begin{pmatrix} \bar{T}_6 & 00 \\ 00 & \bar{T}_6 \end{pmatrix} e^{-j\phi_7} \right\} \begin{pmatrix} Er_{24} \\ Er_{25} \\ Er_{26} \\ Er_{27} \end{pmatrix}$$

$$\begin{aligned}
\begin{pmatrix} Ei_{24} \\ Ei_{25} \\ Ei_{26} \\ Ei_{27} \end{pmatrix} &= e^{-j\phi_7} \begin{pmatrix} Ei_{16} \\ Ei_{17} \\ Ei_{18} \\ Ei_{19} \end{pmatrix} = e^{-j\phi_7} \left\{ \begin{pmatrix} \bar{T}_6 & 0 \\ 0 & 0 \\ 0 & 0 \\ t & \bar{T}_6 \end{pmatrix} \begin{pmatrix} Ei_{12} \\ Ei_{13} \end{pmatrix} + \begin{pmatrix} \bar{C}_6 & 00 \\ 00 & \bar{C}_6 \end{pmatrix} \begin{pmatrix} Ei_{16} \\ Ei_{17} \\ Ei_{18} \\ Ei_{19} \end{pmatrix} \right\} \\
&= e^{-j\phi_7} \begin{pmatrix} \bar{T}_6 & 0 \\ 0 & 0 \\ 0 & \bar{T}_6 \end{pmatrix} \left[ \bar{I}_{2 \times 2} - \bar{C}_4 e^{-j2\phi_5} \begin{pmatrix} S_6^0 & 0 \\ 0 & S_6^0 \end{pmatrix} \right]^{-1} \\
&e^{-j\phi_5} \left[ \bar{T}_4 e^{-j\phi_5} + \bar{C}_4 e^{-j\phi_5} \begin{pmatrix} \bar{T}_6 & 00 \\ 00 & \bar{T}_6 \end{pmatrix} e^{-j\phi_7} \begin{pmatrix} Er_{24} \\ Er_{25} \\ Er_{26} \\ Er_{27} \end{pmatrix} \right] \\
&+ \begin{pmatrix} \bar{C}_6 & 00 \\ 00 & \bar{C}_6 \end{pmatrix} e^{-j\phi_7} \begin{pmatrix} Er_{24} \\ Er_{25} \\ Er_{26} \\ Er_{27} \end{pmatrix}
\end{aligned}$$

$\bar{S}_{11}$  can be written as :

$$\begin{aligned}
S_{11}^{00} &= e^{-j\phi_3} \left\{ e^{-j\phi_3} S_4^{00} + \bar{T}_4 e^{-j\phi_5} \begin{pmatrix} S_6^{00} & 0 \\ 0 & S_6^{00} \end{pmatrix} \right. \\
&\left. \left[ \bar{I}_{2 \times 2} - \bar{C}_4 e^{-j2\phi_5} \begin{pmatrix} S_6^{00} & 0 \\ 0 & S_6^{00} \end{pmatrix} \right]^{-1} \times e^{-j\phi_5} \bar{T}_4 e^{-j\phi_3} \right\}
\end{aligned}$$

$$\begin{aligned}
\bar{T}_{11} &= T_4 e^{-j(\phi_3 + \phi_5)} \left\{ \begin{pmatrix} S_6^{00} & 0 \\ 0 & S_6^{00} \end{pmatrix} \left[ \bar{I}_{2 \times 2} - \bar{C}_4 e^{-j2\phi_5} \begin{pmatrix} S_6^{00} & 0 \\ 0 & S_6^{00} \end{pmatrix} \right]^{-1} \right. \\
&\left. e^{-j2\phi_5} \bar{C}_4 \times \begin{pmatrix} \bar{T}_6 & 00 \\ 00 & \bar{T}_6 \end{pmatrix} e^{-j\phi_7} + \begin{pmatrix} \bar{T}_6 & 00 \\ 00 & \bar{T}_6 \end{pmatrix} e^{-j\phi_7} \right\}
\end{aligned}$$



$$\bar{T}_{11} = e^{-j\phi_7} \begin{pmatrix} T_6 & 0 \\ 0 & T_6 \\ 0 & 0 \end{pmatrix} \left[ \bar{1}_{2 \times 2} - \bar{C}_4 e^{-j2\phi_5} \begin{pmatrix} S_6^{00} & 0 \\ 0 & S_6^{00} \end{pmatrix} \right]^{-1} e^{-j\phi_5} \bar{T}_4 e^{-j\phi_3}$$

$$\bar{C}_{11} = e^{-j\phi_7} \begin{pmatrix} \bar{T}_6 & 0 \\ 0 & \bar{T}_6 \\ 0 & 0 \end{pmatrix} \left[ \bar{1}_{2 \times 2} - \bar{C}_4 e^{-j2\phi_5} \begin{pmatrix} S_6^{00} & 0 \\ 0 & S_6^{00} \end{pmatrix} \right]^{-1} e^{-j\phi_5} \bar{C}_4 e^{-j\phi_3}$$

$$\begin{pmatrix} \bar{T}_6 & 00 \\ 00 & \bar{T}_6 \end{pmatrix} e^{-j\phi_7} + \begin{pmatrix} \bar{C}_6 & 00 \\ 00 & \bar{C}_6 \\ 00 & 00 \end{pmatrix} e^{-2j\phi_7}$$

ANNEXE 3

For the half upper module the computation is the same than before. There is just to change the index :

4 -> 3	13 -> 15	24 -> 28
7 -> 6	16 -> 20	25 -> 29
8 -> 10	17 -> 21	26 -> 30
9 -> 11	18 -> 22	27 -> 31
12 -> 14	19 -> 23	

And  $\bar{T}_3 \rightarrow \bar{T}_8$  and  $\bar{T}_7 \rightarrow \bar{T}_9$ .

Knowing  $\bar{S}_{11}$  and  $\bar{S}_{12}$  there is to calculate the matrix  $\bar{M}$  (10 x 10) which is given by :

$$\begin{pmatrix} Er_1 \\ Er_5 \\ Ei_{24 \rightarrow 31} \end{pmatrix} = \bar{M} \begin{pmatrix} Ei_1 \\ Ei_5 \\ Er_{24 \rightarrow 31} \end{pmatrix}$$

In the previous chapter the following relations can be deduced :

$$\begin{pmatrix} Er_4 \\ Ei_{24 \rightarrow 27} \end{pmatrix} = {}^{11} \begin{pmatrix} Ei_4 \\ Er_{24 \rightarrow 27} \end{pmatrix}$$

$$\begin{pmatrix} Er_3 \\ Ei_{28 \rightarrow 31} \end{pmatrix} = {}^{12} \begin{pmatrix} Ei_3 \\ Er_{28 \rightarrow 31} \end{pmatrix}$$

Taking into account the 3 dB S.M. :

$$\begin{pmatrix} Er_1 \\ Er_5 \\ Ei_4 \\ Ei_3 \end{pmatrix} = \bar{S}_2 \begin{pmatrix} Ei_1 \\ Ei_5 \\ Er_4 \\ Er_3 \end{pmatrix}$$

With :

$$\bar{S}_2 = \begin{pmatrix} 00 & \bar{T}_2 \\ 00 & 00 \\ \bar{T}_2 & 00 \\ 00 & 00 \end{pmatrix}$$

And :

$$\bar{T}_2 = \frac{\sqrt{2}}{2} \begin{pmatrix} -j & 1 \\ 1 & -j \end{pmatrix}$$

Therefore :

$$\begin{pmatrix} Er_1 \\ Er_5 \end{pmatrix} = \bar{T}_2 \left\{ \begin{pmatrix} S_{11}^{00} & 0 \\ 0 & S_{12}^{00} \end{pmatrix} \begin{pmatrix} Ei_4 \\ Ei_3 \end{pmatrix} + \begin{pmatrix} \bar{T}_{11} & 0000 \\ 0000 & \bar{T}_{11} \end{pmatrix} (Er_{24+31}) \right\}$$

Or :

$$\begin{pmatrix} Ei_4 \\ Ei_3 \end{pmatrix} = \bar{T}_2 \begin{pmatrix} Ei_1 \\ Ei_5 \end{pmatrix}$$

Then :

$$\begin{pmatrix} Er_1 \\ Er_5 \end{pmatrix} = \bar{T}_2 \begin{pmatrix} S_{11}^{00} & 0 \\ 0 & S_{12}^{00} \end{pmatrix} \bar{T}_2 \begin{pmatrix} Ei_1 \\ Ei_5 \end{pmatrix} + \bar{T}_2 \begin{pmatrix} \bar{T}_{11} & 0000 \\ 0000 & \bar{T}_{12} \end{pmatrix} (Er_{24 \rightarrow 31})$$

And :

$$(Ei_{24 \rightarrow 31}) = \begin{pmatrix} 0 \\ \bar{T}_{11} \\ 0 \\ 0 \\ 0 \\ 0 \\ 0 \\ 0 \\ 0 \end{pmatrix} \begin{pmatrix} Ei_4 \\ Ei_3 \end{pmatrix} + \begin{pmatrix} \bar{C}_{11} & \bar{O}_{4 \times 4} \\ \bar{O}_{4 \times 4} & \bar{C}_{12} \end{pmatrix} (Er_{24 \rightarrow 31})$$

Then  $\bar{M}$  can be written as :

$$\left[ \begin{array}{cc} \bar{T}_2 \begin{pmatrix} S_{11}^{00} & 0 \\ 0 & S_{12}^{00} \end{pmatrix} \bar{T}_2 & \bar{T}_2 \begin{pmatrix} \bar{T}_{11} & 0000 \\ 0000 & \bar{T}_{12} \end{pmatrix} \\ \begin{pmatrix} 0 \\ \bar{T}_{11} \\ 0 \\ 0 \\ 0 \\ 0 \\ 0 \\ 0 \\ 0 \end{pmatrix} \bar{T}_2 & \begin{pmatrix} \bar{C}_{11} & \bar{O}_{4 \times 4} \\ \bar{O}_{4 \times 4} & \bar{C}_{12} \end{pmatrix} \end{array} \right]$$

On the 3 dB coupler balance port a short-circuit or a load can be put. Noting :

$Ei_5 = \rho_5 Er_5$  and  $\bar{N}$  the 9 x 9 module.

$$\bar{M} = \begin{pmatrix} M^{00} & M^{01} & \bar{M} \\ M^{10} & M^{11} & \bar{M}' \\ \bar{M} & \bar{M}' & \bar{C} \end{pmatrix}$$

$\bar{M}$  is given by :

$$\begin{pmatrix} Er_1 \\ Er_5 \\ Ei_{24 \rightarrow 31} \end{pmatrix} = \bar{M} \begin{pmatrix} Ei_1 \\ Ei_5 \\ Er_{24 \rightarrow 31} \end{pmatrix}$$

$Er_5$  and  $Ei_5$  must be eliminated.

$$Er_5 = M^{10} Ei_1 + M^{11} Ei_5 + \bar{M}' (Er_{24 \rightarrow 31})$$

$$Er_5 = \frac{1}{1 - \rho_5 M^{11}} \{ M^{10} Ei_1 + \bar{M}' (Er_{24 \rightarrow 31}) \}$$

$$Er_1 = M^{00} Ei_1 + M^{01} \rho_5 Er_5 + \bar{M} (Er_{24 \rightarrow 31})$$

$$Er_1 = \left[ M^{00} + \frac{M^{01} M^{10} \rho_5}{1 - \rho_5 M^{11}} \right] Ei_1 + \left[ \frac{M^{01} \rho_5 \bar{M}'}{1 - \rho_5 M^{11}} + \bar{M} \right] (Er_{24 \rightarrow 31})$$

And :

$$\begin{aligned} (Ei_{24 \rightarrow 31}) &= \bar{M} Ei_1 + \bar{M}' \rho_5 Er_5 + \bar{C} (Er_{24 \rightarrow 31}) \\ &= \bar{M} Ei_1 + \frac{\bar{M}' \rho_5}{1 - \rho_5 M^{11}} [M^{10} Ei_1 + \bar{M}' (Er_{24 \rightarrow 31})] \\ &\quad + \bar{C} (Er_{24 \rightarrow 31}) \end{aligned}$$

$$(Ei_{24 \rightarrow 31}) = \left[ \bar{M} + \frac{\bar{M}' \rho_s}{1 - \rho_s M^{11}} M^{10} \right] Ei_1 + \left\{ \frac{\bar{M}' \rho_s}{1 - \rho_s M^{11}} \bar{M}' + \bar{C} \right\} (Er_{24 \rightarrow 31})$$

The matrix  $\bar{N}'$  can be written as :

$$\begin{pmatrix} M^{00} + \frac{M^{01} M^{10}}{1 - \rho_s M^{11}} \rho_s & \frac{M^{01} \rho_s \bar{M}'}{1 - \rho_s M^{11}} + \bar{M} \\ \bar{M} + \frac{\bar{M}' \rho_s M^{10}}{1 - \rho_s M^{11}} & \frac{\bar{M}' \rho_s \bar{M}'}{1 - \rho_s M^{11}} + \bar{C} \end{pmatrix}$$

Remarks :

the antenna S.M.

For each module  $i$  the scattering matrix is now known  $\bar{S}_i$ , the antenna S.M. is given by :

$$\begin{pmatrix} \bar{S}_1 & 0 \\ 0 & \bar{S}_{16} \end{pmatrix}$$

ANNEXE 4



Notation :

As in the previous chapter  $\bar{N}$  is the matrix of 1 module.

The antenna is made of 2 rows of 8 modules therefore the matrix of half the antenna  $\bar{T}$  can be defined as :

$$\bar{T} = \begin{pmatrix} \bar{N}_{11} & & & 0 \\ & \cdot & & \\ & & \cdot & \\ 0 & & & \bar{N}_{88} \end{pmatrix}$$

$$((\bar{T})) = 72 \times 72$$

The electric fields are defined as  $\bar{V}'_1$  and  $\bar{V}''_1$ . They are linked together by the relation :

$$\bar{V}''_1 = \bar{T} \bar{V}'_1$$

With :

$$\bar{V}'_1 = \begin{array}{l} \left| \begin{array}{l} V'_{11} \\ V'_{12} \\ \cdot \\ \cdot \\ V'_{19} \\ \cdot \\ \cdot \end{array} \right. \end{array} \quad \begin{array}{l} \leftarrow \text{input port} \\ \\ \\ \text{module n}^\circ 1 \end{array}$$

Noting :

$$\overline{W}'_2 = \begin{array}{l} \left| \begin{array}{l} V''_{12} \\ \cdot \\ \cdot \\ V''_{19} \\ \cdot \\ \cdot \\ \cdot \\ V''_{82} \\ V''_{89} \end{array} \right. \end{array} \quad \begin{array}{l} \\ \\ \\ \text{1st module} \\ \\ \\ \\ \\ \text{8th module} \end{array}$$

and

$$\overline{W}''_2 = \begin{array}{l} \left| \begin{array}{l} V'_{12} \\ \cdot \\ \cdot \\ V'_{19} \\ \cdot \\ \cdot \\ \cdot \\ V'_{82} \\ V'_{89} \end{array} \right. \end{array}$$

With the code SWAN (Slow Wave ANTenna) the plasma matrix can be deduced for one row of 32 waveguides. The incident field, the density and the density gradient must be known. Therefore the matrix  $P_0$  is corresponding to one half of 8 modules. If the coupling in the poloidal direction is supposed negligible to have the matrix corresponding to the 8 whole modules  $P$ , the relation which give  $P$  is :

$$\bar{P} = \begin{pmatrix} \bar{M}_{11} & \bar{O} & \bar{M}_{12} & \dots & \bar{M}_{18} & \bar{O} \\ \bar{O} & \bar{M}_{11} & \bar{O} & \dots & & \\ \cdot & & & & & \\ \cdot & & & & & \\ \cdot & & & & & \\ \bar{M}_{81} & & & & & \end{pmatrix}$$

With :

$$\bar{P}_0 = \begin{pmatrix} \bar{M}_{11} & \bar{M}_{12} & \dots & \bar{M}_{18} \\ \cdot & & & \\ \cdot & & & \\ \cdot & & & \\ \bar{M}_{81} & & & \bar{M}_{88} \end{pmatrix}$$

The size of  $\bar{M}$  and  $\bar{O}$  are (4 x 4). Therefore the size of  $\bar{P}$  is 64 x 64.

The following relation then can be written :

$$\bar{W}''_2 = \bar{P} \bar{W}'_2$$

$\bar{T}$  can be written as :

$$\begin{pmatrix} S_{11} & \bar{T}_{11} & & & \\ & & \bar{O} & & \\ \bar{T}_{11} & \bar{C}_{12} & & & \\ & & & S_{12} & \bar{T}_{22} & \dots \\ & & & \bar{T}_{22} & \bar{C}_{22} & \dots \end{pmatrix}$$

It can be deduced that :

$$\begin{pmatrix} \bar{T}_{11} & 0 \\ 0 & \bar{T}_{88} \end{pmatrix} \begin{pmatrix} V'_{11} \\ \vdots \\ V'_{81} \end{pmatrix} + \begin{pmatrix} \bar{C}_{11} & 0 \\ 0 & \bar{C}_{88} \end{pmatrix} \begin{pmatrix} \bar{V}'_{1 \ 2 \rightarrow 9} \\ \vdots \\ \bar{V}'_{8 \ 2 \rightarrow 9} \end{pmatrix} = \begin{pmatrix} \bar{V}''_{1 \ 2 \rightarrow 9} \\ \vdots \\ \bar{V}''_{8 \ 2 \rightarrow 9} \end{pmatrix}$$

We have also :

$$\begin{pmatrix} V'_{1 \ 2 \rightarrow 9} \\ \vdots \\ V'_{8 \ 2 \rightarrow 9} \end{pmatrix} = \begin{pmatrix} V''_{1 \ 2 \rightarrow 9} \\ \vdots \\ V''_{8 \ 2 \rightarrow 9} \end{pmatrix}$$

Therefore :

$$\begin{pmatrix} V''_{1 \ 2 \rightarrow 9} \\ \vdots \\ V''_{8 \ 2 \rightarrow 9} \end{pmatrix} = \begin{pmatrix} \bar{T}_{11} & \\ & \bar{T}_{88} \end{pmatrix} \begin{pmatrix} \bar{V}'_{11} \\ \vdots \\ \bar{V}'_{81} \end{pmatrix} + \begin{pmatrix} \bar{C}_{11} & \\ & \bar{C}_{88} \end{pmatrix} \bar{P} \begin{pmatrix} V''_{1 \ 2 \rightarrow 9} \\ \vdots \\ V''_{8 \ 2 \rightarrow 9} \end{pmatrix}$$

It can be deduced that :

$$\begin{pmatrix} V''_{1 \ 2 \rightarrow 9} \\ \vdots \\ V''_{8 \ 2 \rightarrow 9} \end{pmatrix} = \left\{ \bar{I}_{64 \times 64} - \begin{pmatrix} \bar{C}_{11} & 0 \\ 0 & \bar{C}_{88} \end{pmatrix} \bar{P} \right\}^{-1} \begin{pmatrix} \bar{T}_{11} & \\ & \bar{T}_{88} \end{pmatrix} \begin{pmatrix} \bar{V}'_{11} \\ \vdots \\ \bar{V}'_{81} \end{pmatrix}$$

Who have also :

$$\begin{pmatrix} \bar{V}'_{1 \ 2 \rightarrow 9} \\ \vdots \\ \bar{V}'_{8 \ 2 \rightarrow 9} \end{pmatrix} = \begin{pmatrix} V''_{1 \ 2 \rightarrow 9} \\ \vdots \\ V''_{8 \ 2 \rightarrow 9} \end{pmatrix}$$

The total electric field at the end of the antenna in front of the plasma is given by :

$$\begin{pmatrix} \bar{V}'_{1 \ 2 \rightarrow 9} \\ \cdot \\ \cdot \\ \bar{V}'_{8 \ 2 \rightarrow 9} \end{pmatrix} + \begin{pmatrix} \bar{V}''_{1 \ 2 \rightarrow 9} \\ \cdot \\ \cdot \\ \bar{V}''_{8 \ 2 \rightarrow 9} \end{pmatrix}$$

The reflected field at the input of the modules is given by :

$$\begin{pmatrix} V''_{11} \\ \cdot \\ \cdot \\ V''_{81} \end{pmatrix} = \begin{pmatrix} S_{11} & & & \\ & \cdot & & \\ & & \cdot & \\ & & & S_{81} \end{pmatrix} \begin{pmatrix} V'_{11} \\ \cdot \\ \cdot \\ V'_{81} \end{pmatrix} + \begin{pmatrix} \bar{T}_{11} & & & \\ & \cdot & & \\ & & \cdot & \\ & & & \bar{T}_{81} \end{pmatrix} \begin{pmatrix} \bar{V}'_{1 \ 2 \rightarrow 9} \\ \cdot \\ \cdot \\ \bar{V}'_{3 \ 2 \rightarrow 9} \end{pmatrix}$$

From the previous relation the total electric field can be injected into SWAN to compute the  $N''$  spectra. Therefore during the experiment, knowing :

- The density and the density gradient at the mouth of the antenna.
- The incident field at the input of each module the real  $N//$  spectra injected can be computed.
- And the computed reflected field can be compared to the measured one.
- The coupling coefficient at the input of each module can be deduced when one module alone is fed by the klystron. The coupling coefficients are then given by :

$$S_{ij} = V''_{ij} / V'_{ij}$$

PHOTO 1  
ONE ANTENNA MOUTH INSIDE TORE SUPRA



PHOTO 2

THE MODULE PROTOTYPE AND THE LOADS AT THE BOTTOM  
WHICH WERE USED DURING THE MEASUREMENT

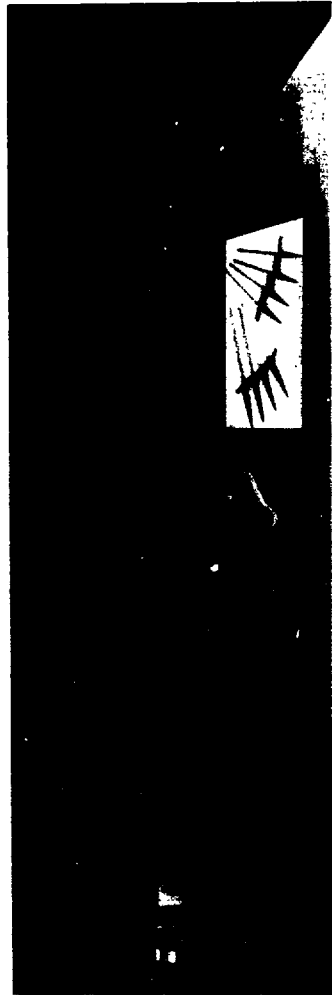


PHOTO 3  
THE EXCITING MAGNETIC LOOP

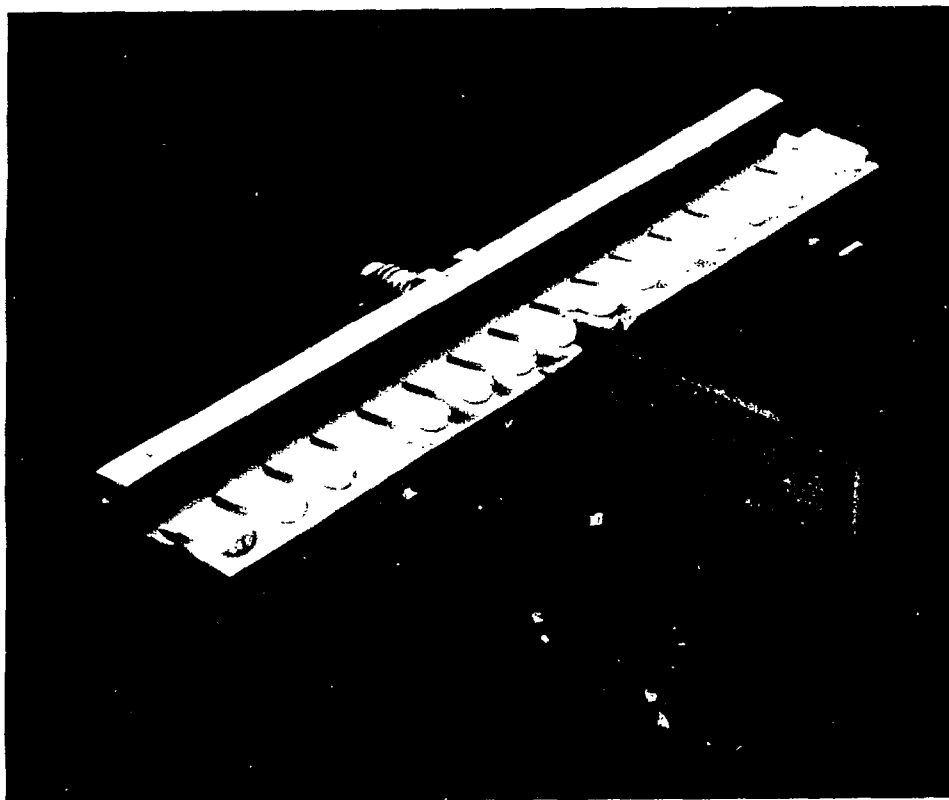
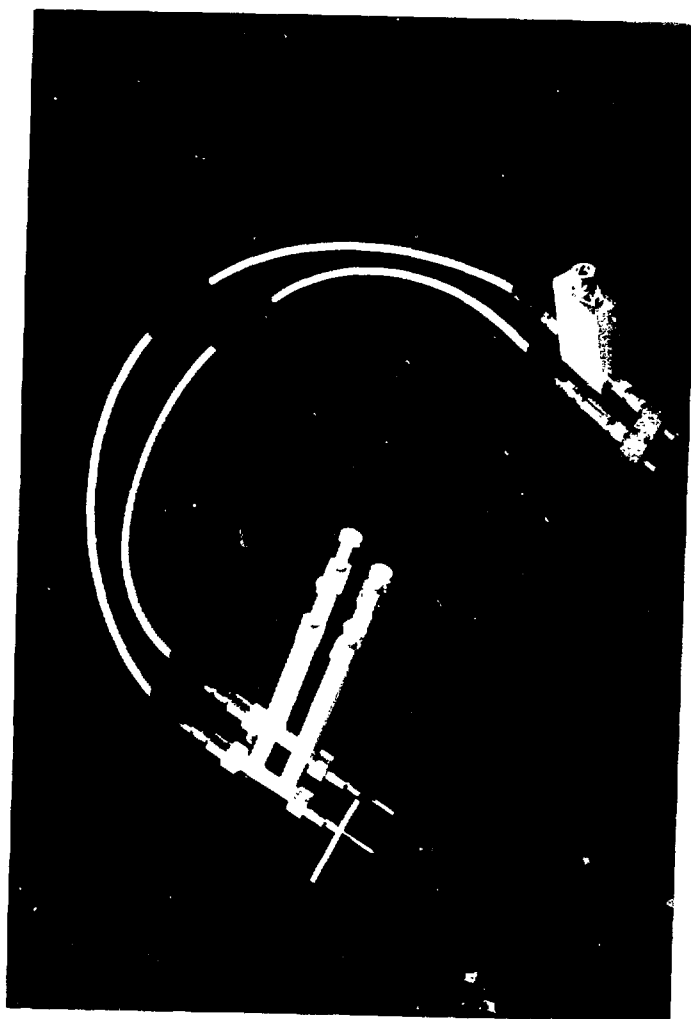




PHOTO 4  
THE PROBES FOR THE MEASUREMENT OF THE INCIDENT  
AND REFLECTED WAVE INSIDE THE REDUCED WAVEGUIDE



	0	1	2	3	4	5	6	7	8
0	5,638.10 <sup>-2</sup> 6,9	0,3524 - 31,2	0,3524 58,8	0,3524 148,8	0,3524 - 121,2	0,3524 - 31,2	0,3524 58,8	0,3524 148,8	0,3524 - 121,2
1	0,3524 - 31,2	0,504 102,6	0,612 - 40,8	0,247 - 157,4	0,247 - 67,4	0	0	0	0
2	0,3524 58,8	0,612 - 40,8	0,504 - 77,4	0,247 - 67,4	0,247 22,6	0	0	0	0
3	0,3524 148,8	0,247 - 157,4	0,247 - 67,4	0,504 102,6	0,612 - 40,8	0	0	0	0
4	0,3524 - 121,2	0,247 - 67,4	0,247 22,6	0,612 - 40,8	0,504 - 77,4	0	0	0	0
5	0,3524 - 31,2	0	0	0	0	0,504 102,6	0,612 - 40,8	0,247 - 157,4	0,247 - 67,4
6	0,3524 58,8	0	0	0	0	0,612 - 40,8	0,504 - 77,4	0,247 - 67,4	0,247 22,6
7	0,3524 148,8	0	0	0	0	0,247 - 157,4	0,247 - 67,4	0,504 102,6	0,612 - 40,8
8	0,3524 - 121,2	0	0	0	0	0,247 - 67,4	0,247 22,6	0,612 - 40,8	0,504 - 77,4

TAB 1  
THEORETICAL MATRIX OF THE MODULE PROTOTYPE WITH  
A LOAD ON THE BALANCE PORT OF THE 3 dB COUPLER

	0	1	2	3	4	5	6	7	8
0	5,638.10 <sup>-2</sup> 6,9	0,3524 - 31,2	0,3524 58,8	0,3524 148,8	0,3524 - 121,2	0,3524 - 31,2	0,3524 58,8	0,3524 148,8	0,3524 - 121,2
1	0,3524 - 31,2	0,578 92	0,495 - 38	0,372 - 152	0,372 - 62	0,118 - 136	0,118 - 46	0,118 44	0,118 134
2	0,3524 58,8	0,495 - 38	0,578 - 88	0,372 - 62	0,372 28	0,118 - 46	0,118 44	0,118 134	0,118 - 136
3	0,3524 148,8	0,372 - 152	0,372 - 62	0,578 92	0,495 - 38	0,118 44	0,118 134	0,118 - 136	0,118 - 46
4	0,3524 - 121,2	0,372 - 62	0,372 28	0,495 - 38	0,578 - 88	0,118 134	0,118 - 136	0,118 - 46	0,118 44
5	0,3524 - 31,2	0,118 - 136	0,118 - 46	0,118 44	0,118 134	0,578 92	0,495 - 38	0,372 - 152	0,372 - 62
6	0,3524 58,8	0,118 - 46	0,118 44	0,118 134	0,118 - 136	0,495 - 38	0,578 - 88	0,372 - 62	0,372 28
7	0,3524 148,8	0,118 44	0,118 134	0,118 - 136	0,118 - 46	0,372 - 152	0,372 - 62	0,578 92	0,495 - 38
8	0,3524 - 121,2	0,118 134	0,118 - 136	0,118 - 46	0,118 44	0,372 - 62	0,372 28	0,495 - 38	0,578 - 88

TAB 2  
THEORETICAL SCATTERING MATRIX OF THE MODULE PROTOTYPE WITH  
A SHORT-CIRCUIT ON THE BALANCE PORT OF THE 3 dB COUPLER

	0	1	2	3	4	5	6	7	8	10
0	0,03	0,35	0,35	0,35	0,35	0,35	0,35	0,35	0,35	$7 \cdot 10^{-5}$
1		0,5	0,62	0,25	0,25					0,35
2			0,5	0,25	0,25					0,35
3				0,5	0,62					0,35
4					0,5					0,35
5						0,5	0,62	0,25	0,25	0,35
6							0,5	0,25	0,25	0,35
7								0,5	0,62	0,35
8									0,5	0,35
10										0,03

TAB 3  
THEORETICAL 10 X 10 MATRIX  
AMPLITUDE FOR THE MODULE 0 AND TYPE 1H, 1B, 2H, 2B

	0	1	2	3	4	5	6	7	8	10	76
0	+ 116	- 137	- 49	+ 47	+ 133	- 137	- 49	+ 47	+ 133	+ 6	
1		+ 139	- 4	- 144	- 54					+ 158	
2			- 44	- 54	+ 38					- 112	
3				+ 139	- 4					- 20	
4					- 44					+ 70	
5						+ 139	- 4	- 144	- 54	- 20	
6							- 44	- 54	+ 38	+ 70	
7								+ 139	- 4	+ 164	
8									- 44	- 106	
10										- 10	

TAB 4  
THEORETICAL 10 x 10 MATRIX  
PHASE FOR THE MODULE 0

	0	1	2	3	4	5	6	7	8	10
0	+131	- 42	+ 46	+ 141	- 124	- 42	+ 46	+ 142	- 124	+ 121
1	- 101	-100	+ 110	- 25	+ 65					+ 82
2	- 13	- 160	+76	+ 65	+ 160					+ 172
3	+ 76	+ 66	+ 160	-100	+ 110					- 88
4	+ 167	+ 160	- 110	- 160	+76					+ 2
5	- 101				+ 170	-13	- 160	+ 66	+160	- 98
6	- 13					-100	+170	+ 160	- 110	- 8
7	+ 76					+ 110	+76	+ 160	- 110	- 8
8	+ 167					- 25	+ 65	-14	- 160	+ 88
10	- 167	+ 40	+ 130	- 140	- 48	- 140	- 48	+ 40	+ 130	+ 34

TAB 5  
THEORETICAL 10 X 10 MATRIX  
PHASES FOR THE MODULES TYPE 1H, 1B

	0	1	2	3	4	5	6	7	8	10
0	-54 +34	- 143	- 58	+ 43	+ 133	+ 37	+ 127	- 137	- 48	- 167
1	- 98	-100 -13	+ 110	- 25	+ 65					- 111
2	- 8	- 160	+76 +170	+ 65	+ 160					- 16
3	+ 88	+ 66	+ 160	-100 -14	+ 110					+ 79
4	+ 178	+ 160	- 110	- 160	+76 + 170					+ 170
5	+ 82					-13 -100	- 160	+ 66	+160	+ 111
6	172					+ 110	+170 +76	+ 160	- 110	- 16
7	- 88					- 25	+ 65	-14 -100	- 160	+ 79
8	+ 2					+ 65	+ 160	+ 110	+170 + 76	+ 170
10	+ 122	- 42	+ 48	+ 144	- 122	- 42	+ 48	+ 144	- 124	+ 1 +131

**TAB 6**  
**THEORETICAL 10 x 10 MATRIX**  
**PHASES FOR THE MODULES TYPE 2H, 2B**

0,03	0,35	0,35	0,35	0,35	0,35	0,35	0,35	0,35
	0,392	0,639	0,347	0,347	0,126	0,126	0,126	0,126
		0,392	0,347	0,347	0,126	0,126	0,126	0,126
			0,392	0,639	0,126	0,126	0,126	0,126
				0,392	0,126	0,126	0,126	0,126
					0,451	0,746	0,175	0,175
						0,451	0,175	0,175
							0,451	0,746
								0,451

+ 131	- 42	+ 48	+ 138	- 132	- 42	+ 48	+ 138	- 132
	- 108	+ 121	- 41	+ 49	- 73	+ 17	+ 107	- 163
		+ 72	+ 49	+ 139	+ 17	+ 107	- 163	- 73
			- 108	+ 121	+ 107	- 163	- 73	+ 17
				+ 72	- 163	- 73	+ 17	+ 107
					+ 1	- 160	+ 38	+ 128
						- 179	+ 128	- 142
							+ 1	- 161
								- 179

TAB 7  
THEORETICAL AMPLITUDE AND PHASE OF THE 9 x 9  
SCATTERING MATRIX OF A 1H MODULE



0,03	0,35	0,35	0,35	0,35	0,35	0,35	0,35	0,35
	0,612	0,612	0,206	0,206	0,121	0,121	0,121	0,121
		0,612	0,206	0,206	0,121	0,121	0,121	0,121
			0,612	0,612	0,121	0,121	0,121	0,121
				0,612	0,121	0,121	0,121	0,121
					0,471	0,739	0,168	0,168
						0,471	0,168	0,168
							0,471	0,739
								0,471

+ 1	- 101	- 11	+ 79	+ 169	- 101	- 11	+ 79	+ 169
	- 8	- 171	+ 95	- 175	- 169	+ 79	+ 11	+ 101
		+ 171	- 175	- 85	- 79	+ 11	+ 101	- 169
			- 8	- 171	+ 11	+ 101	- 169	- 79
				+ 171	+ 108	- 169	- 79	+ 11
					- 86	+ 108	- 50	+ 40
						+ 94	+ 40	+ 130
							- 86	+ 108
								+ 94

TAB 8  
THEORETICAL AMPLITUDE AND PHASE OF THE 9 x 9  
SCATTERING MATRIX OF A 1B MODULE

	0	1	2	3	4	5	6	7	8
0	0,0841 137	0,325 - 35	0,305 53	0,374 143	0,367 - 118	0,331 - 38	0,341 64	0,389 119	0,325 - 145
1	0,378 - 35	0,498 121	0,63 - 26	0,277 - 143	0,242 - 44	0,0167 - 13	0,012 85	0,0146 136	0,0134 - 127
2	0,371 59	0,616 - 23	0,427 - 59	0,266 - 51	0,253 44	0,0117 77	0,012 - 175	0,0123 - 92	0,0119 - 37
3	0,389 144	0,251 - 148	0,245 - 54	0,484 104	0,631 - 24	0,0139 - 173	0,012 - 95	0,0195 - 22	0,0113 53
4	0,384 - 124	0,244 - 61	0,251 + 36	0,668 - 28	0,38 - 69	0,0131 - 103	0,0151 - 5	0,0195 48	0,0216 159
5	0,333 - 34	0,013 - 23	0,01 94	0,0158 177	0,015 - 87	0,378 132	0,603 - 23	0,272 - 160	0,214 - 57
6	0,346 53	0,029 67	0,0149 - 176	0,0186 - 87	0,015 - 7	0,668 - 12	0,429 - 37	0,29 - 70	0,215 33
7	0,342 128	0,0148 138	0,0168 - 116	0,0178 - 33	0,0188 70	0,238 - 140	0,223 - 55	0,398 98	0,585 - 37
8	0,338 - 133	0,0157 - 125	0,0158 - 31	0,0168 57	0,0211 145	0,236 - 55	0,218 35	0,699 - 45	0,592 - 60

TAB 9  
EXPERIMENTAL MATRIX OF THE MODULE PROTOTYPE WITH A LOAD

	0	1	2	3	4	5	6	7	8
0	0,0851 139	0,3408 - 35	0,3349 62	0,3589 165	0,3349 249	0,3672 - 22	0,3254 68	0,363 134	0,3162 223
1	0,3449 - 35	0,6531 109	0,5217 - 28	0,3427 -139	0,2867 - 61	0,1102 - 93	0,1047 5	0,1266 78	0,0846 170
2	0,3521 59	0,5956 - 33	0,4144 - 67	0,363 - 37	0,3002 37	0,1065 8	0,0988 104	0,1237 170	0,0971 - 90
3	0,3605 144	0,378 - 134	0,33 - 39	0,5495 108	0,5188 - 41	0,1041 102	0,1059 - 159	0,123 - 98	0,0971 0
4	0,3591 231	0,3408 - 50	0,2985 30	0,6095 - 37	0,5308 - 72	0,1011 - 175	0,1047 - 79	0,1174 - 10	0,0865 88
5	0,3464 - 44	0,1141 - 96	0,0988 3	0,1258 100	0,0971 - 169	0,4954 103	0,5011 - 23	0,3958 - 143	0,2834 - 45
6	0,3646 54	0,1195 -3	0,1065 99	0,1273 - 163	0,1035 - 81	0,5623 - 27	0,4097 - 72	0,3912 - 50	0,3002 51
7	0,3591 138	0,1128 70	0,1011 175	0,1216 - 88	0,0994 6	0,3507 - 144	0,3254 - 45	0,6309 107	0,6025 - 29
8	0,3563 225	0,1096 162	0,1035 - 98	0,1216 0	0,1122 84	0,3527 - 57	0,3198 46	0,5688 -13	0,5128 - 89

TAB 10  
EXPERIMENTAL MATRIX OF THE MODULE PROTOTYPE WITH A SHORT-CIRCUIT

	0	1	2	3	4	5	6	7	8	10
0	0,03	0,37	0,31	0,37	0,33	0,37	0,3	0,38	0,33	0,05
1	0,34	0,44	0,63	0,29	0,26					0,36
2	0,32	0,65	0,46	0,27	0,25					0,36
3	0,35	0,27	0,26	0,43	0,67					0,37
4	0,32	0,27	0,25	0,66	0,43					0,35
5	0,35					0,05	0,69	0,27	0,25	0,37
6	0,34					0,6	0,43	0,26	0,23	0,36
7	0,35					0,26	0,24	0,5	0,68	0,34
8	0,33					0,24	0,22	0,68	0,51	0,33
10	0,05	0,33	0,35	0,32	0,34	0,33	0,33	0,32	0,34	0,08

TAB 11  
EXPERIMENTAL 10 x 10 MATRIX  
AMPLITUDE FOR THE MODULE "0"

	0	1	2	3	4	5	6	7	8	10
0	+ 177°	- 145	- 51	+ 44	+ 134	- 141	- 46	+ 37	+ 135	- 13
1	- 149	+ 140	+ 3	- 129	- 36					+ 159
2	- 52	+ 6	- 28	- 29	+ 61					- 10
3	+ 37	- 130	- 38	+ 154	+ 12					- 13
4	+ 134	- 35	+ 57	+ 19	- 27					+ 79
5	- 133					+ 154	- 6	- 119	- 25	- 11
6	- 40					+ 12	- 29	- 25	+ 68	+ 76
7	+ 40					- 116	- 22	+ 150	- 2	+ 166
8	+ 134					- 24	+ 69	+ 14	- 27	- 101
10	- 13	+ 156	- 108	- 7	+ 79	- 21	+ 75	+ 171	- 110	- 63°

TAB 12  
EXPERIMENTAL 10 x 10 MATRIX  
PHASES FOR THE MODULE "0"

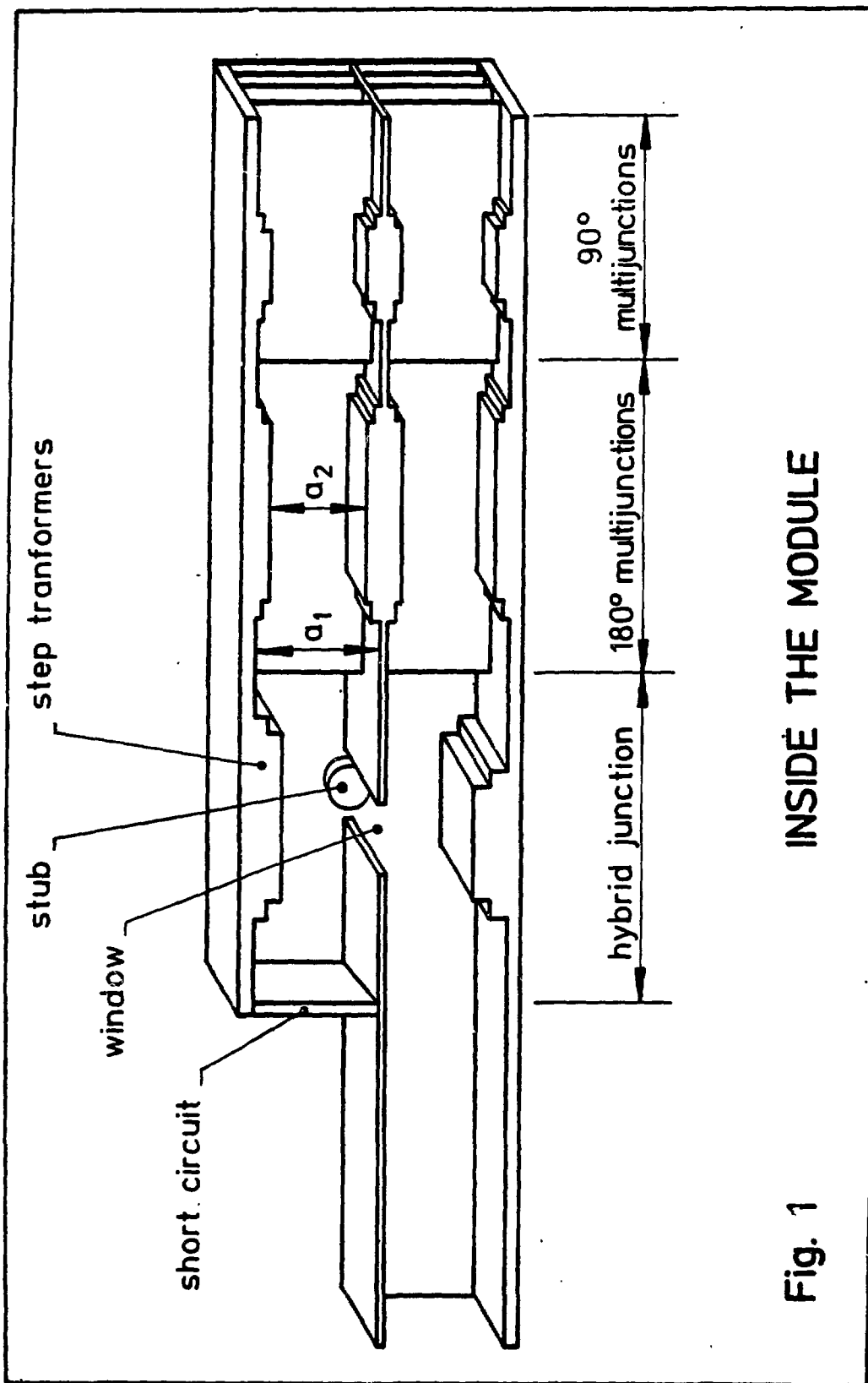


Fig. 1  
INSIDE THE MODULE

### THE DIFFERENT TYPES OF MODULE

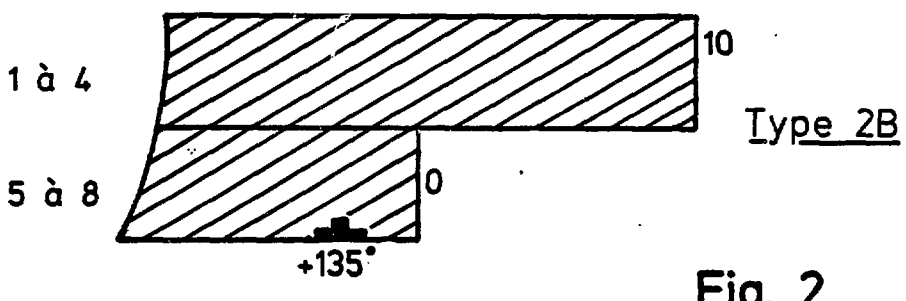
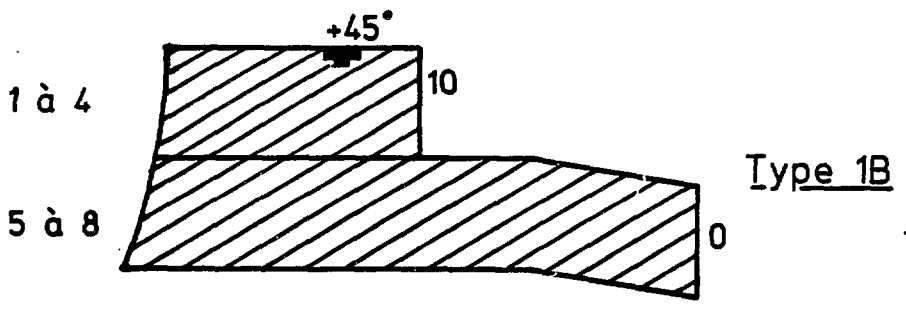
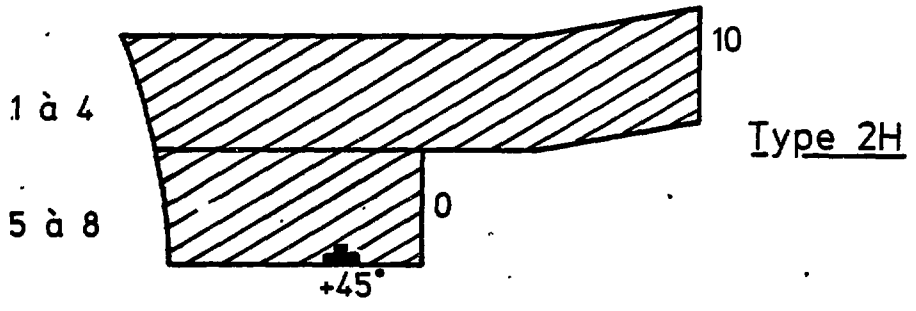
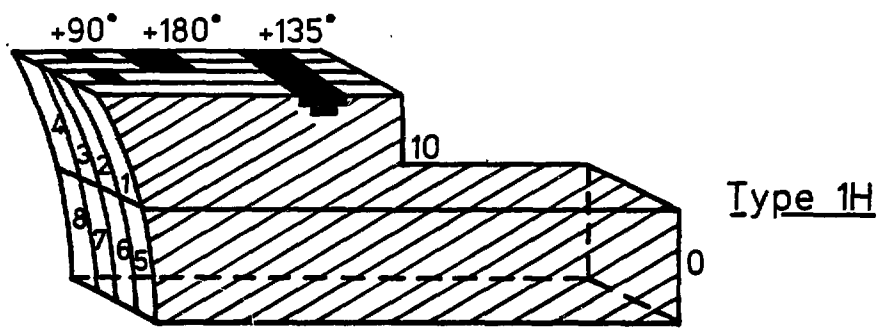
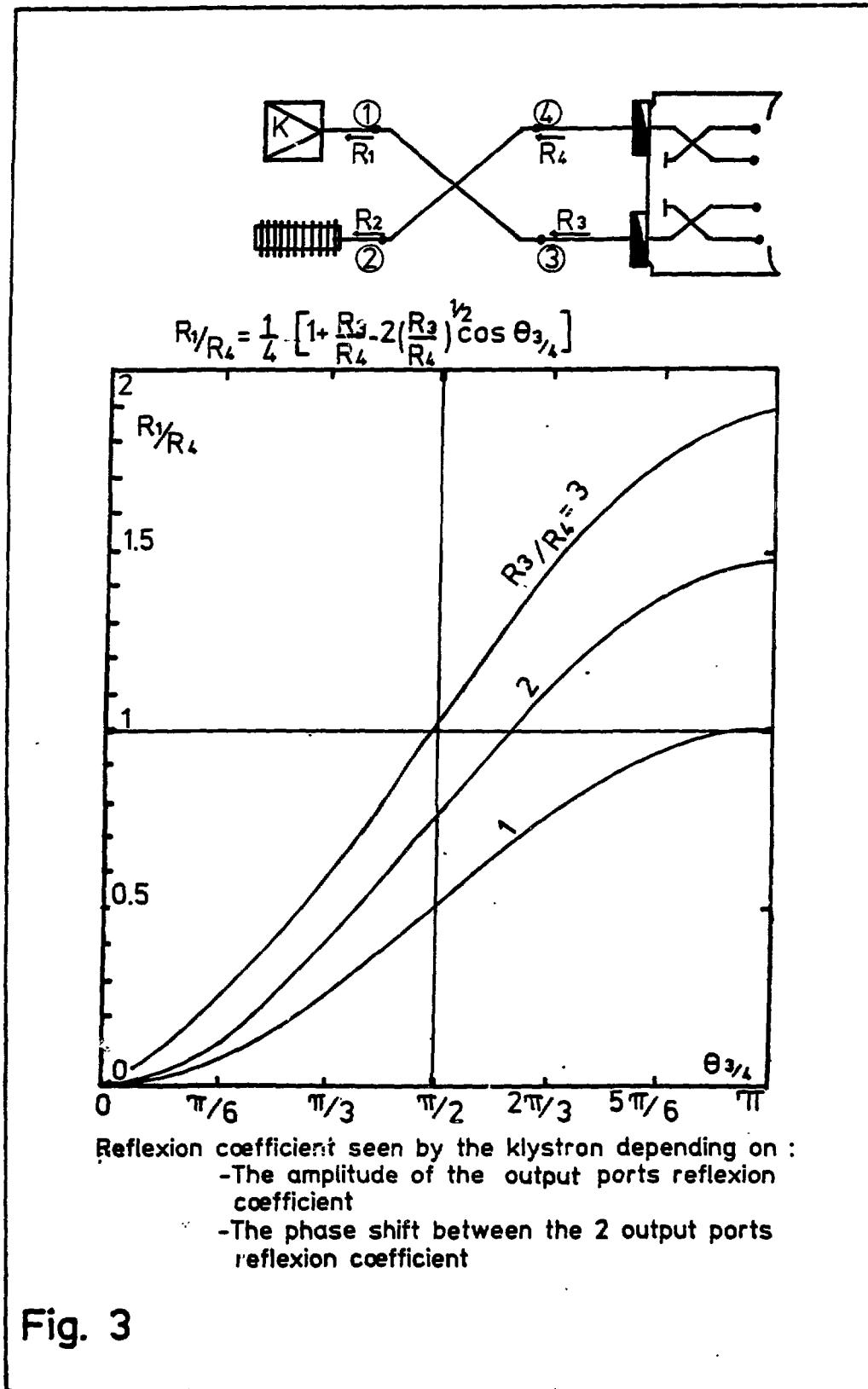


Fig. 2





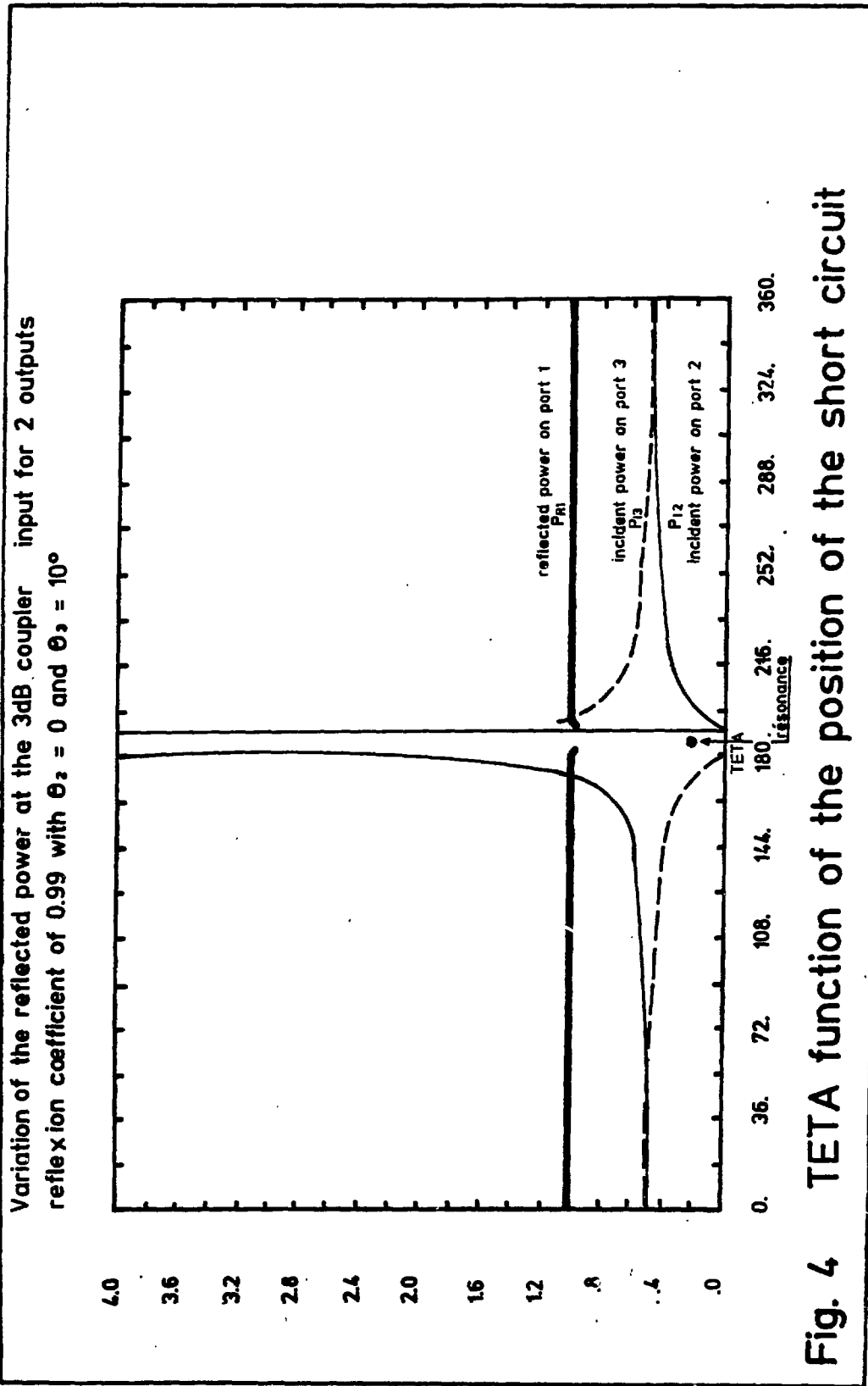


Fig. 4 TETA function of the position of the short circuit

0  
1  
2  
3  
4  
5  
6  
7  
8

NUMERATION OF THE DIFFERENT  
WAVEGUIDES AND DISCONTINUITIES

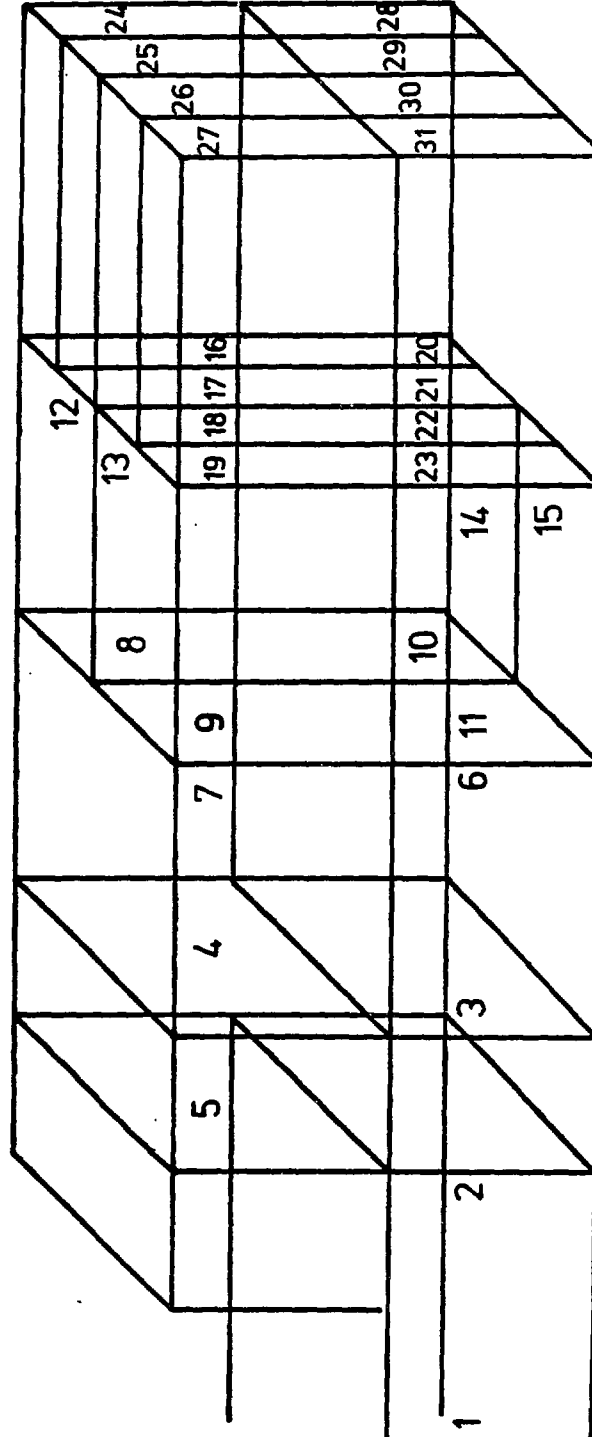


Fig. 5

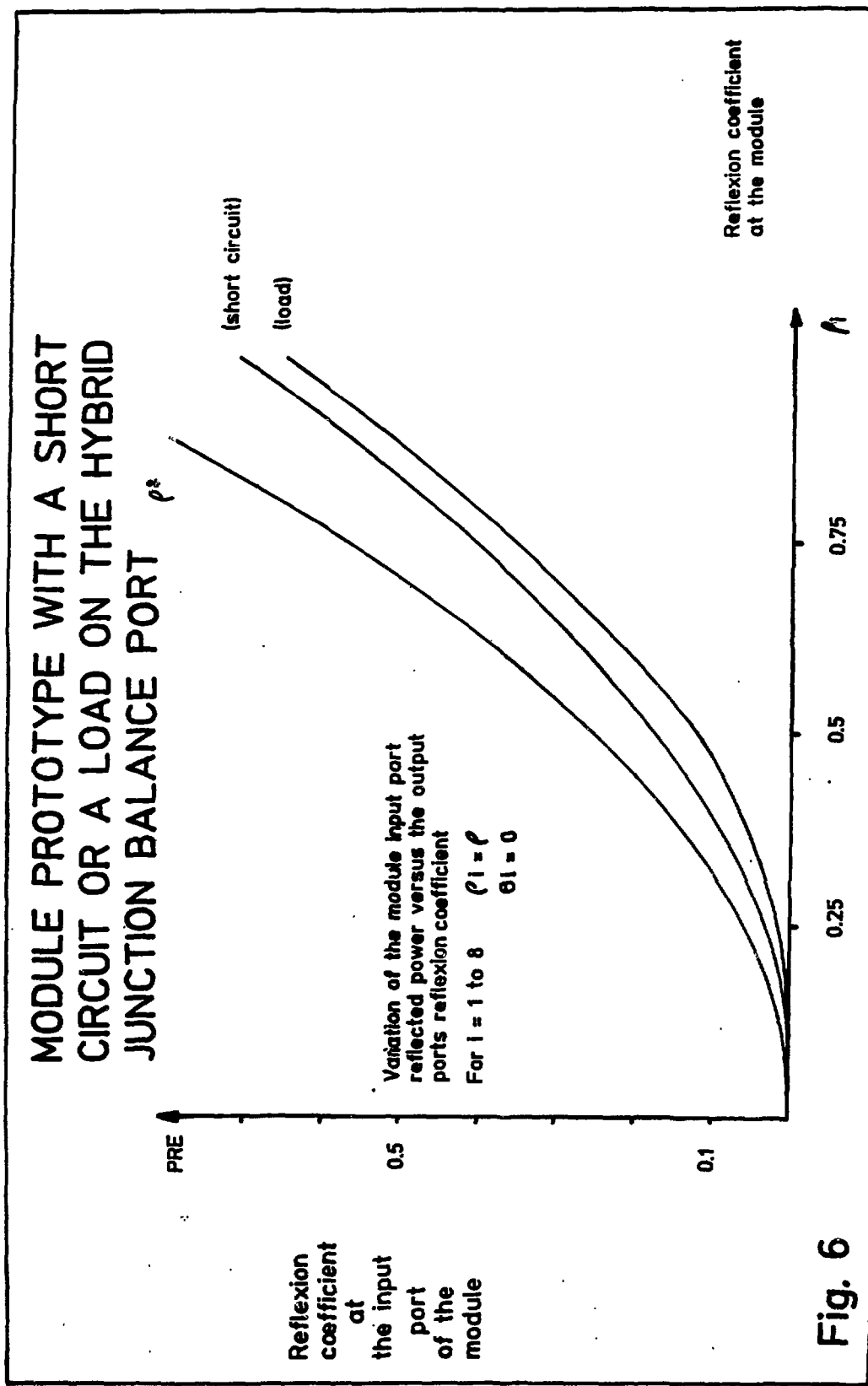


Fig. 6

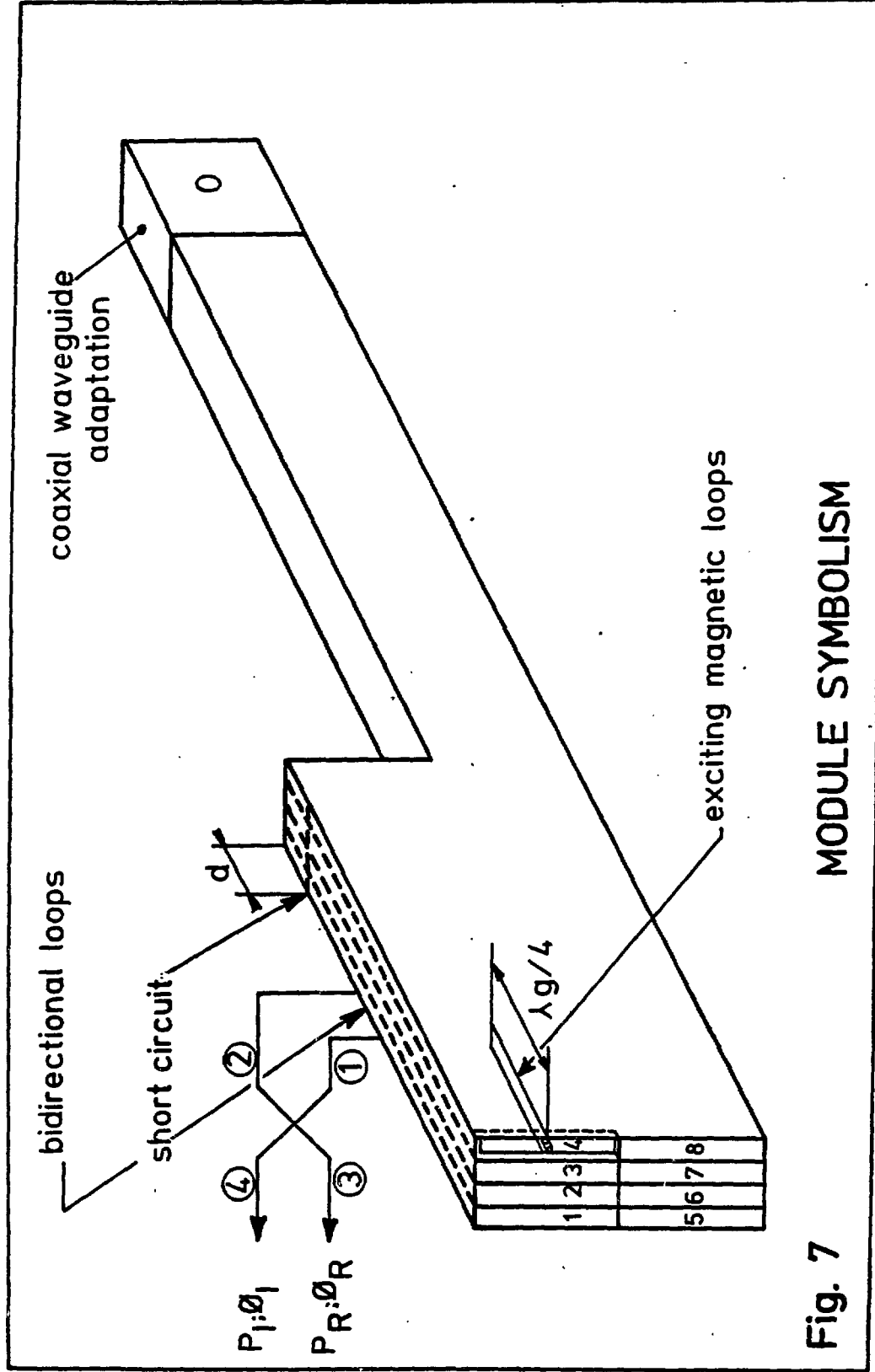


Fig. 7

MODULE SYMBOLISM

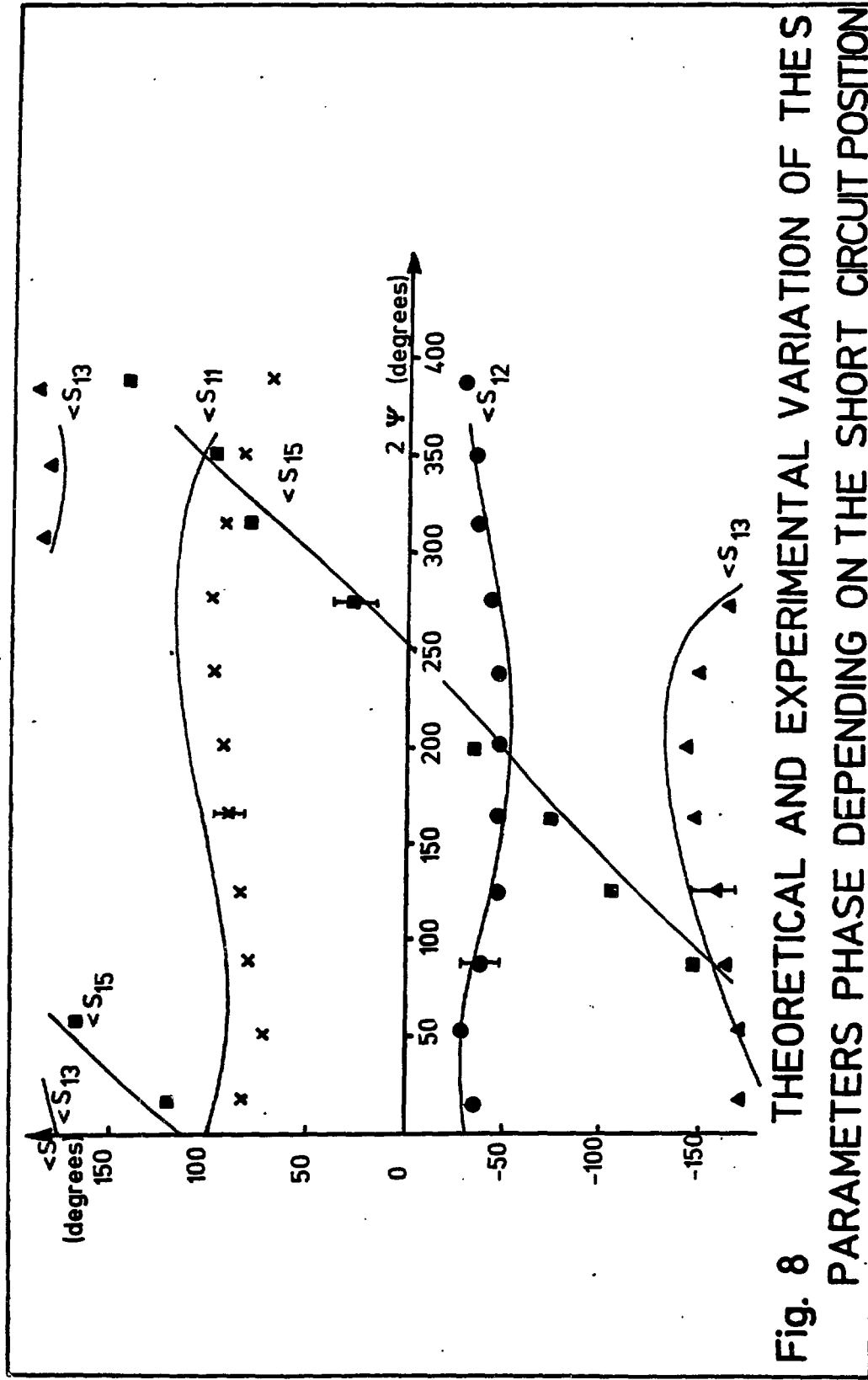


Fig. 8 THEORETICAL AND EXPERIMENTAL VARIATION OF THE SHORT-CIRCUIT PARAMETERS PHASE DEPENDING ON THE SHORT CIRCUIT POSITION

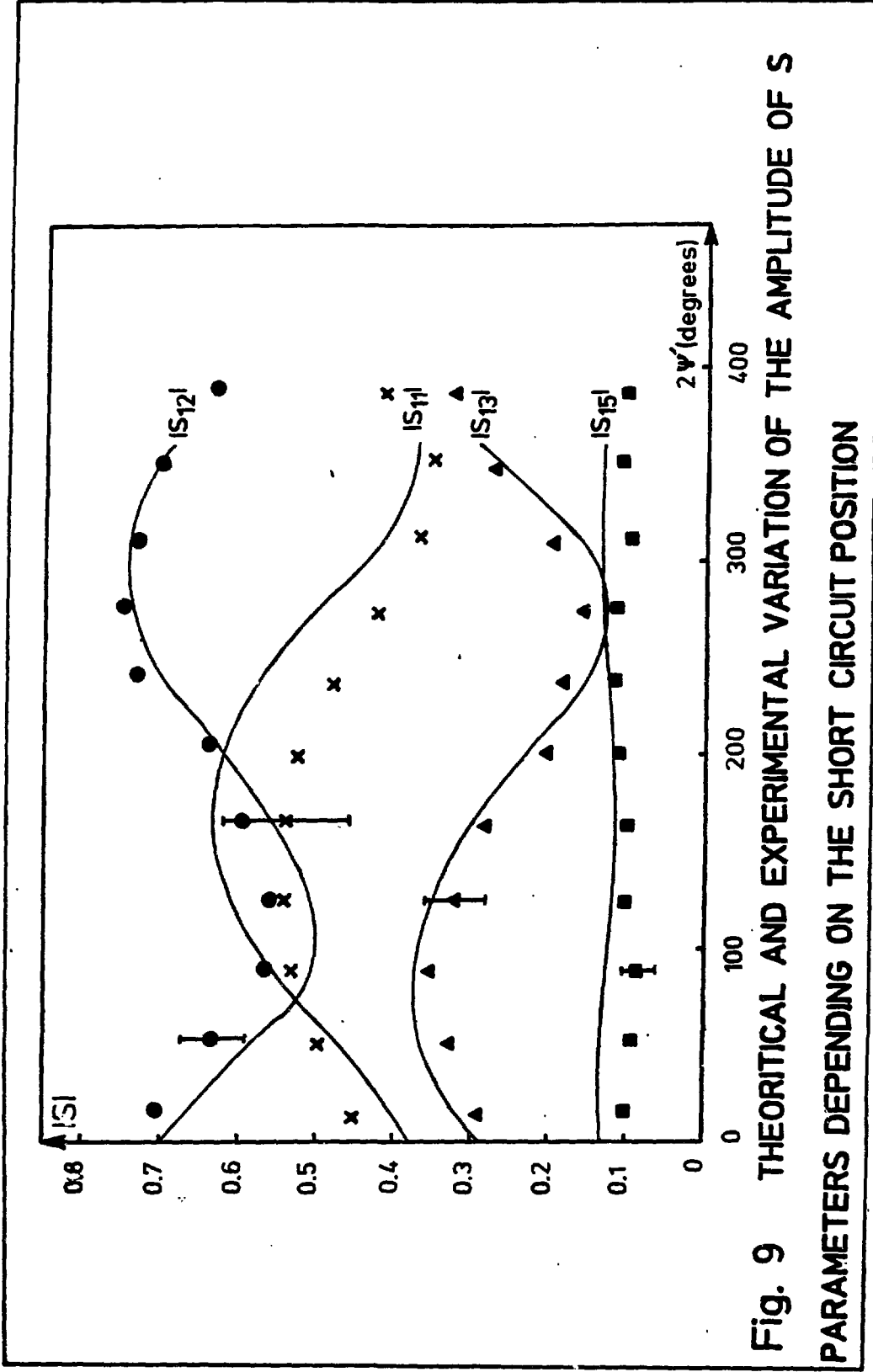
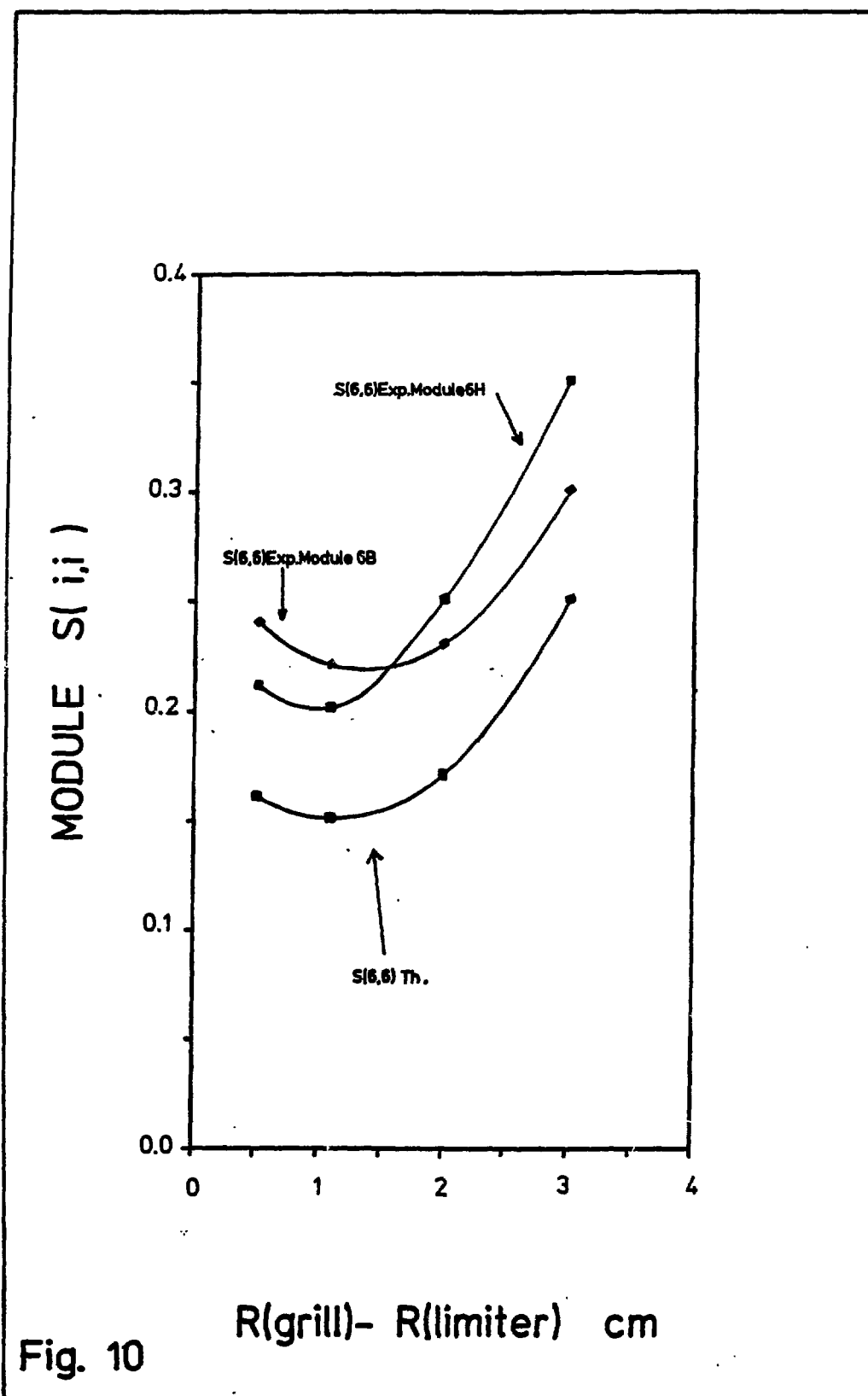
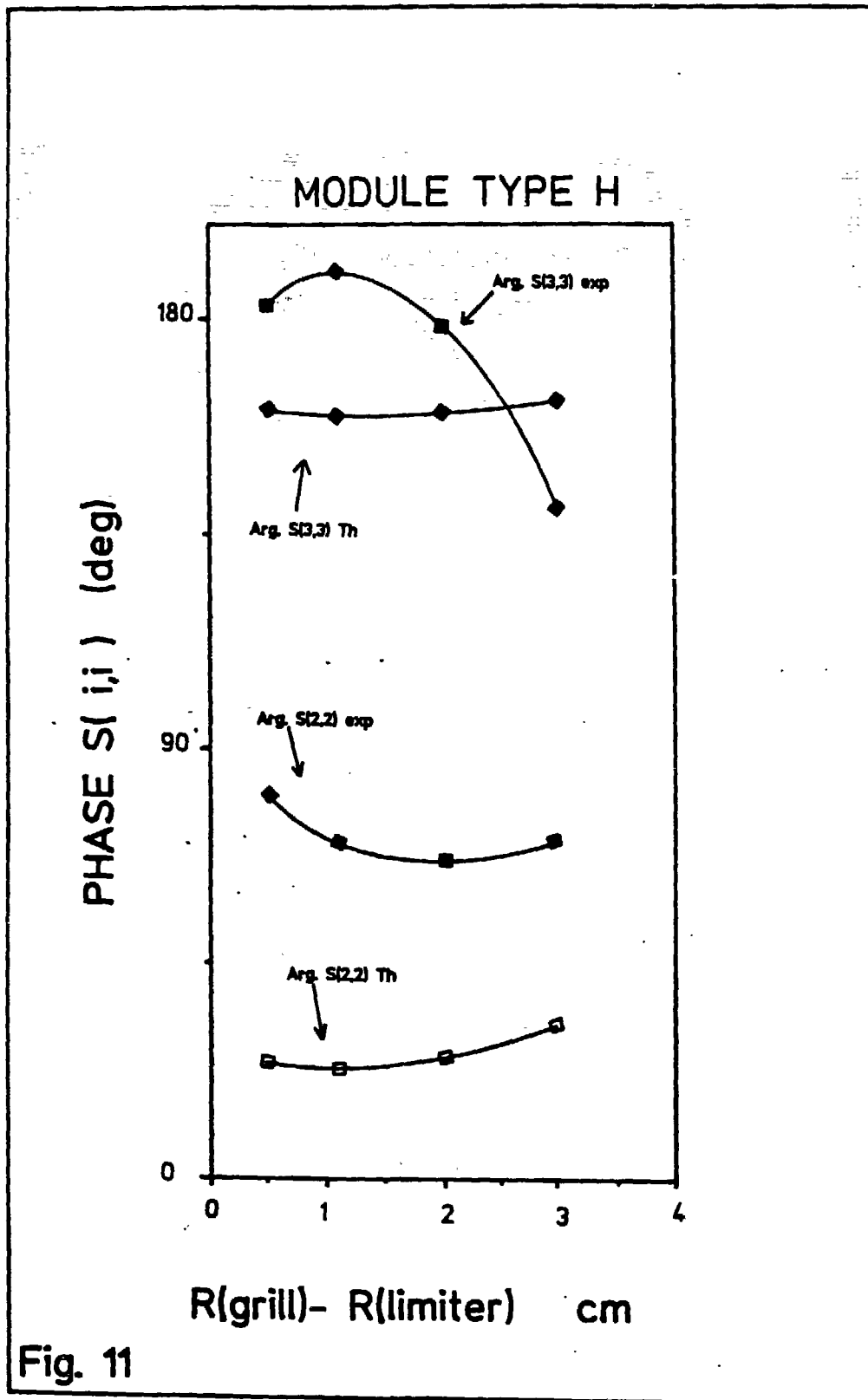


Fig. 9 THEORETICAL AND EXPERIMENTAL VARIATION OF THE AMPLITUDE OF S PARAMETERS DEPENDING ON THE SHORT CIRCUIT POSITION







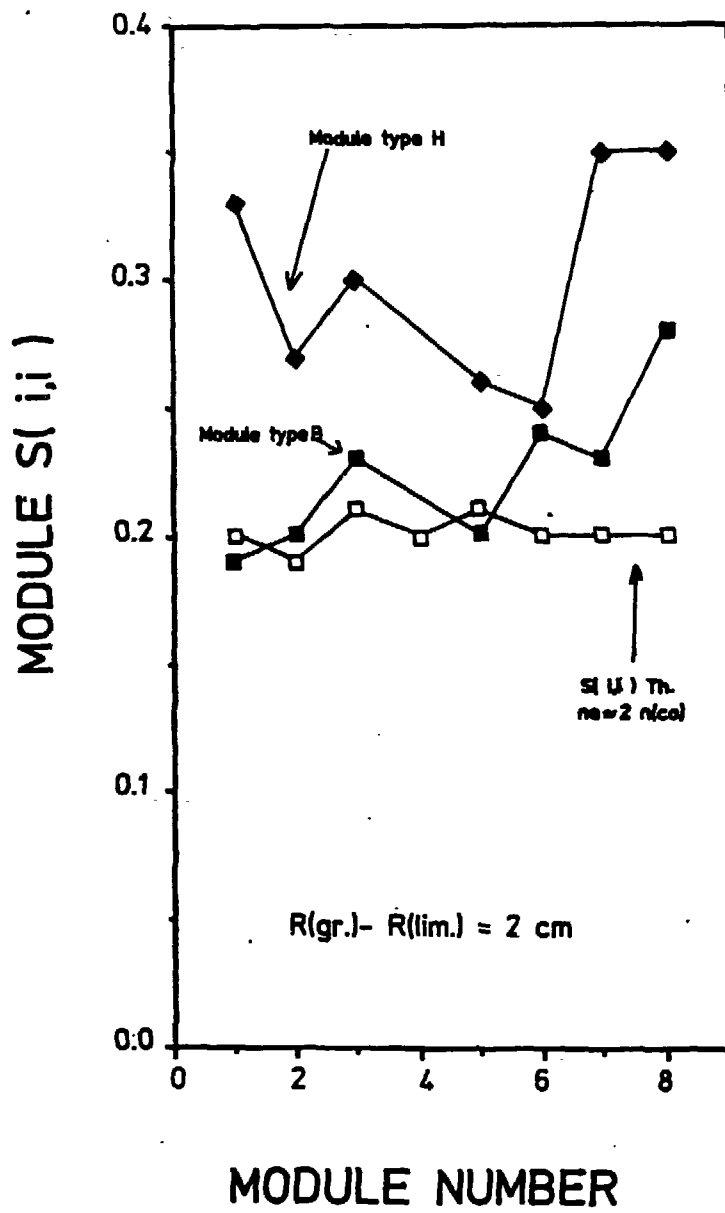


Fig. 12

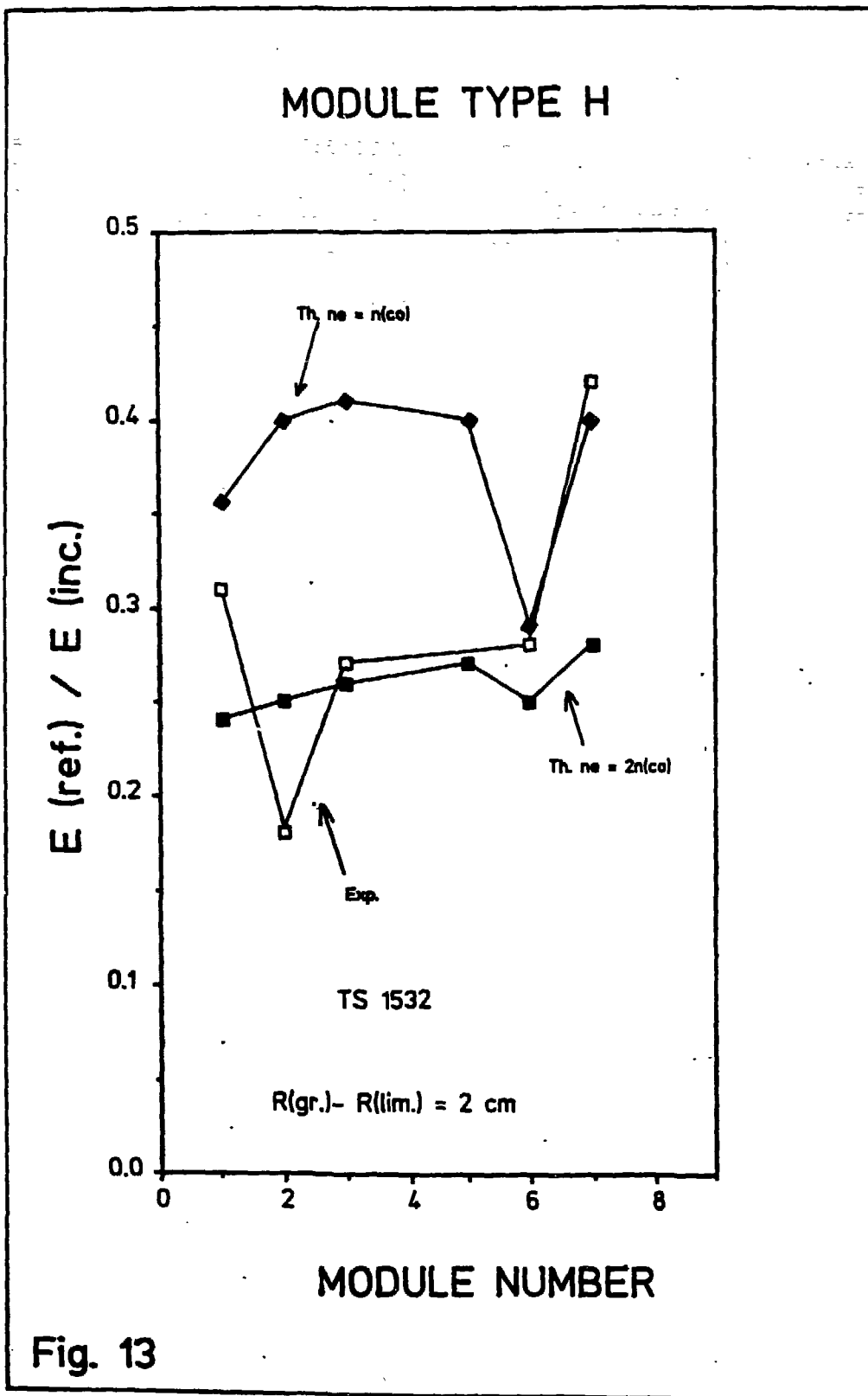
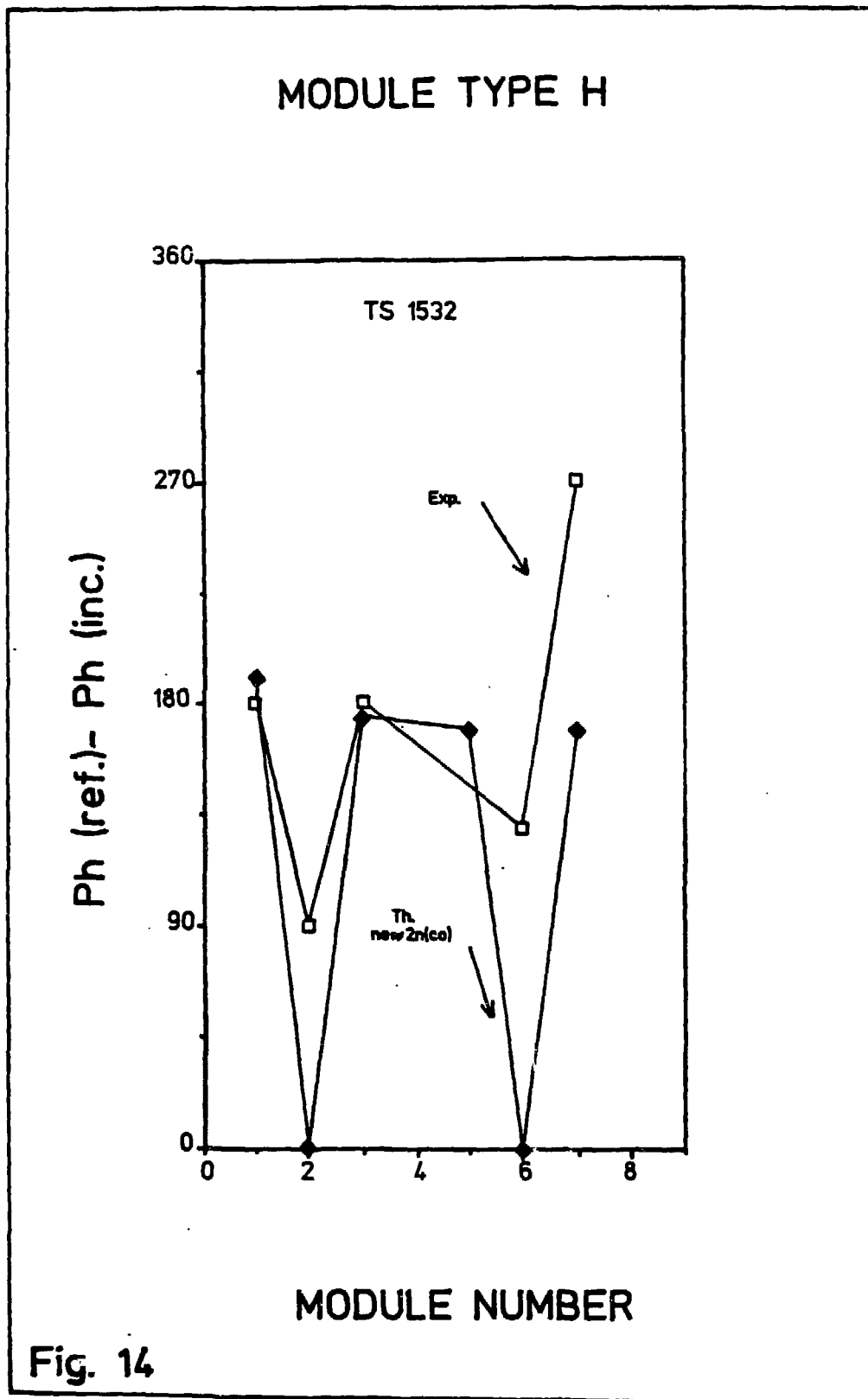
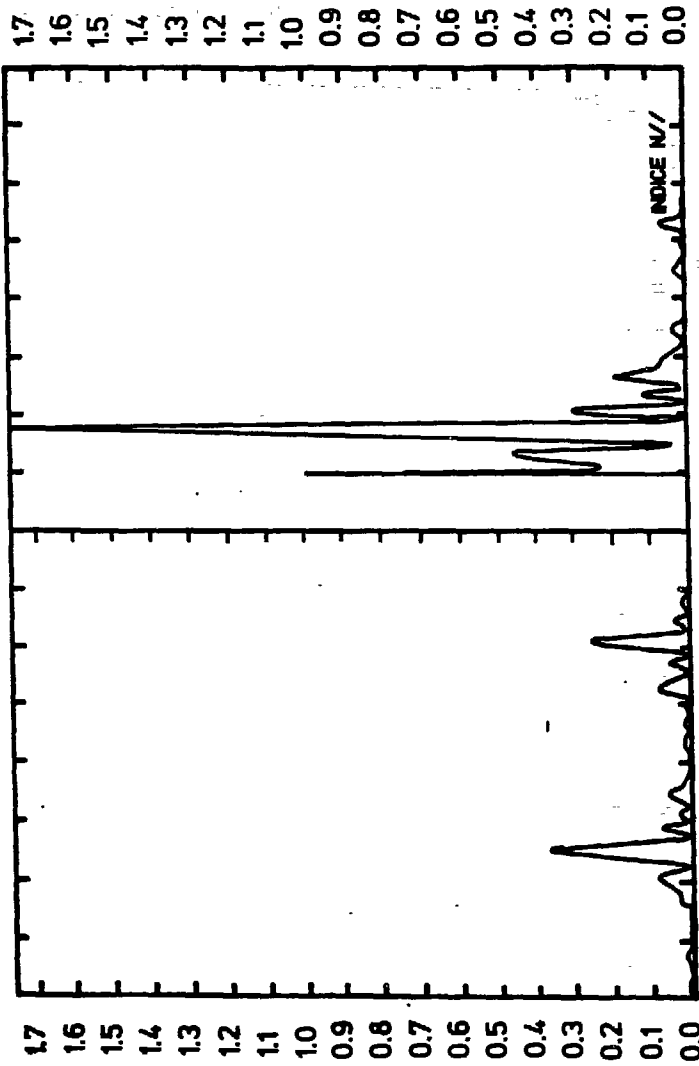


Fig. 13



# EXPERIMENTAL SPECTRA



# POWER SPECTRA / TRANSMITTED POWER

Fig. 15